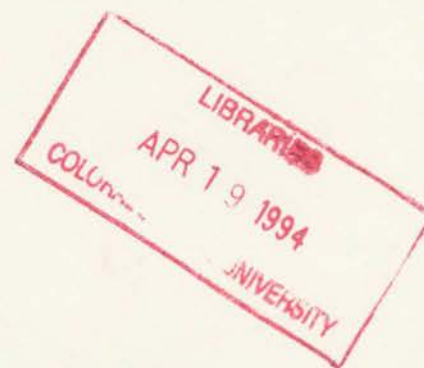


QUALITY CONTROL AND ASSESSMENT OF WIND PROFILER MEASUREMENTS

by: **Paul F. Hein and Stephen K. Cox**
Department of Atmospheric Science
Colorado State University
Fort Collins, CO 80523

Funding Agencies:

Office of Naval Research,
Contract #N00014-91-J-1422, P0004
National Aeronautics & Space Administration,
Contract #NAG-1-1146



**Colorado
State
University**

**DEPARTMENT OF
ATMOSPHERIC SCIENCE**

PAPER NO. 543

**QUALITY CONTROL AND ASSESSMENT
OF WIND PROFILER MEASUREMENTS**

Paul F. Hein and Stephen K. Cox

**Department of Atmospheric Science
Colorado State University
Fort Collins, CO 80523**

Funding Agencies:

**Office of Naval Research,
Contract #N00014-91-J-1422, P0004**

**National Aeronautics & Space Administration,
Contract #NAG-1-1146**

December 1993



U18401 0265220

Atmospheric Science Paper No. 543

QC
852
.C6
no. 543
ATMOS

TABLE OF CONTENTS

1.0	Introduction	1
1.1	The Wind Profiler	1
1.2	Wind Profiler Operation	1
1.3	Limitations	4
2.0	Quality Control Methods	5
2.1	Consensus Averaging	5
2.2	NOAA Network Method	5
2.3	Continuity Method	5
2.4	CSU Method	6
3.0	Beam comparison	6
3.1	Background	6
3.2	Comparison of the Measurements and the Quality Control Methods	7
3.3	Comparison with the Porto Santo Data Set	19
4.0	Finding the Correct Peak in the Doppler Spectrum	23
5.0	Concluding Remarks	34
	References	39

LIST OF FIGURES

Figure 1.	Beam configuration of the wind profiler.	2
Figure 2.	A typical wind profiler doppler spectrum.	3
Figure 3.	The variability of wind profiler data is seen. Note how the effect of the vertical velocity can be removed by using ΔS	8
Figure 4.	A comparison of the east and west beams using the CSU method.	9
Figure 5.	A comparison of the north and south beams using the CSU method.	10
Figure 6.	A comparison of beams using the CSU method: ΔS	11
Figure 7.	A comparison of the east and west beams using the NOAA network method.	13
Figure 8.	A comparison of the north and south beams using the NOAA network method.	14
Figure 9.	A comparison of beams using the NOAA network method: ΔS	15
Figure 10.	A comparison of the east and west beams using the continuity method.	16
Figure 11.	A comparison of the north and south beams using the continuity method.	17
Figure 12.	A comparison of beams using the continuity method: ΔS	18
Figure 13.	A comparison of the east and west beams using the CSU method on data from Porto Santo.	20
Figure 14.	A comparison of the north and south beams using the CSU method on data from Porto Santo.	21
Figure 15.	A comparison of beams using the CSU method on data from Porto Santo: ΔS	22
Figure 16.	The standard peak removal can leave much of the center peak there. The new method of removing the center peak will remove all the center peak, while leaving the only the obvious embedded peaks.	24
Figure 17a.	High wind case on 31 March 1991: Spectra processed by the standard method with standard center peak removal.	26

Figure 17b. High wind case on 31 March 1991: Spectra processed by the standard method with the new center peak removal method.	27
Figure 17c. High wind case on 31 March 1991: Spectra processed by the new method with standard center peak removal.	28
Figure 17d. High wind case on 31 March 1991: Spectra processed by the new method with the new center peak removal method.	29
Figure 18a. Typical case on 23 November 1991: Spectra processed by the standard method with standard center peak removal.	30
Figure 18b. Typical case on 23 November 1991: Spectra processed by the standard method with the new center peak removal method.	31
Figure 18c. Typical case on 23 November 1991: Spectra processed by the new method with standard center peak removal.	32
Figure 18d. Typical case on 23 November 1991: Spectra processed by the new method with the new center peak removal method.	33
Figure 19a. A west wind case on 26 November 1991: Spectra processed by the standard method with standard center peak removal.	35
Figure 19b. A west wind case on 26 November 1991: Spectra processed by the standard method with the new center peak removal method.	36
Figure 19c. A west wind case on 26 November 1991: Spectra processed by the new method with standard center peak removal.	37
Figure 19d. A west wind case on 26 November 1991: Spectra processed by the new method with the new center peak removal method.	38

1.0 Introduction

Remote sensing of the atmospheric winds provides the observer with many advantages as well as some limitations. Wind profiling gives the observer on the ground a high temporal depiction of winds at various heights in the atmosphere. Unfortunately the wind profiler sometimes senses and measures other phenomena besides wind. The removal of these spurious measurements and an assessment of the quality of the measurements that are the foci of this report.

1.1 *The Wind Profiler*

The Colorado State University (CSU) wind profiler is a five beam clear air doppler radar. Four of the five beams are tilted 15° off vertical, mapping out the four points of the compass as seen in Figure 1. The fifth beam is vertical. The CSU wind profiler can measure winds from 500 meters to greater than 15 km above ground level. The wind profiler specifications are described in Table 1.

Table 1.

Manufacturer and Model	Tycho DORA 400S Wind Profiler
Transmit Frequency	404.37 MHz
Radiated Power	40 kW (peak)
Beamwidth	5 degrees
Antenna Type	Phased Array of Coaxial Collinear Dipoles
Antenna Dimensions	12 meters x 12 meters

1.2 *Wind Profiler Operation*

The wind profiler transmits pulses of electromagnetic energy. A small fraction of the transmitted energy is scattered by irregularities in the refractive index of the air, directing a small amount of energy back toward the radar receiver. The movement of air toward or away from the wind profiler will cause a shift in the frequency of the received signal. This doppler shift is proportional to the speed of the air motion along the direction of the beam. From these measured radial velocities a horizontal wind speed and direction can be calculated.

Figure 2 shows a typical power spectrum. The center peak is due to ground clutter and must be removed by software. The average noise level is also subtracted off. The largest peak is chosen and a power-weighted-average of frequency from the peak is then selected and converted from a doppler shifted frequency to a radial velocity.

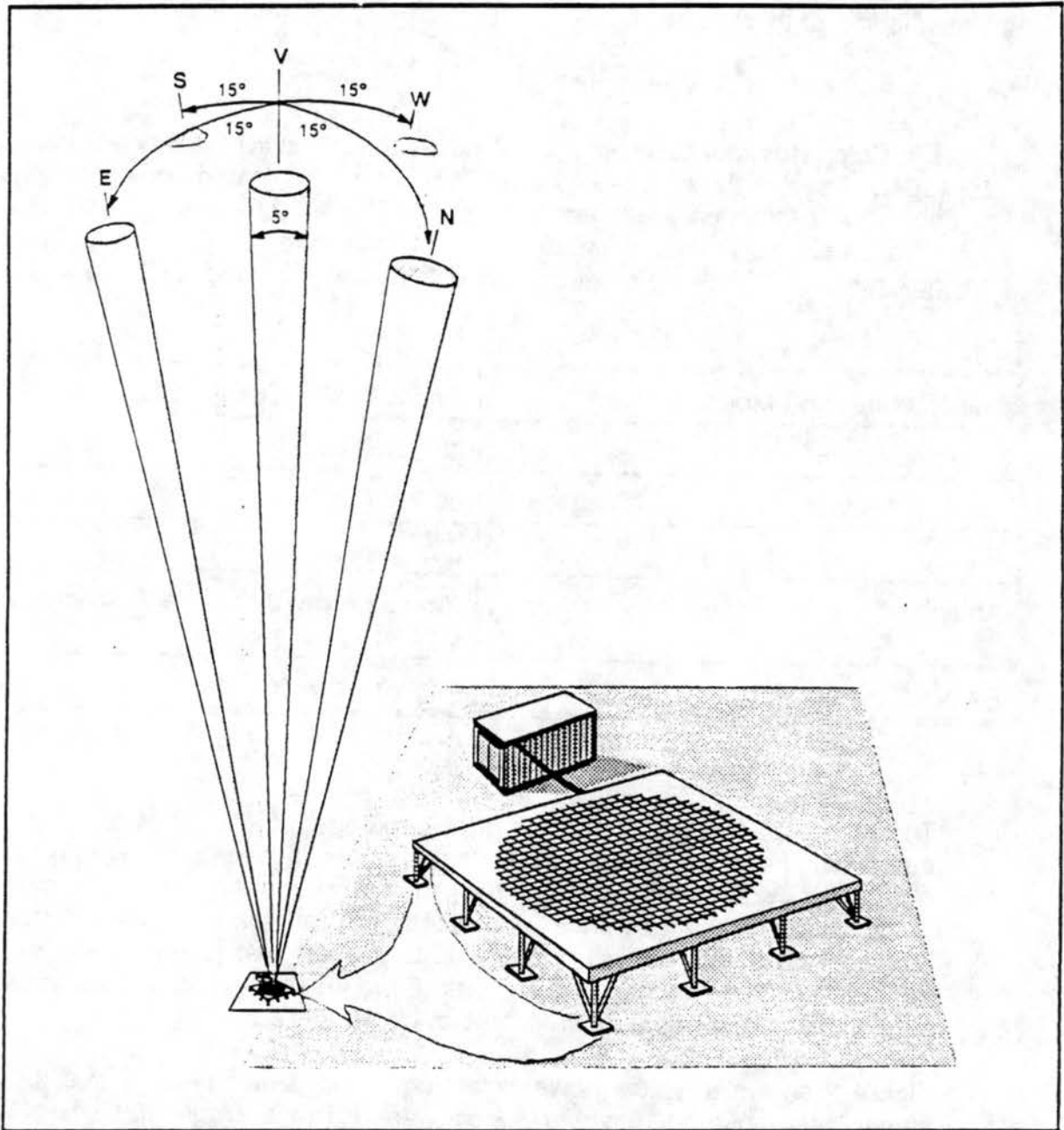


Figure 1. Beam configuration of the wind profiler.

CSU Wind Profiler: 911123 0214 Z

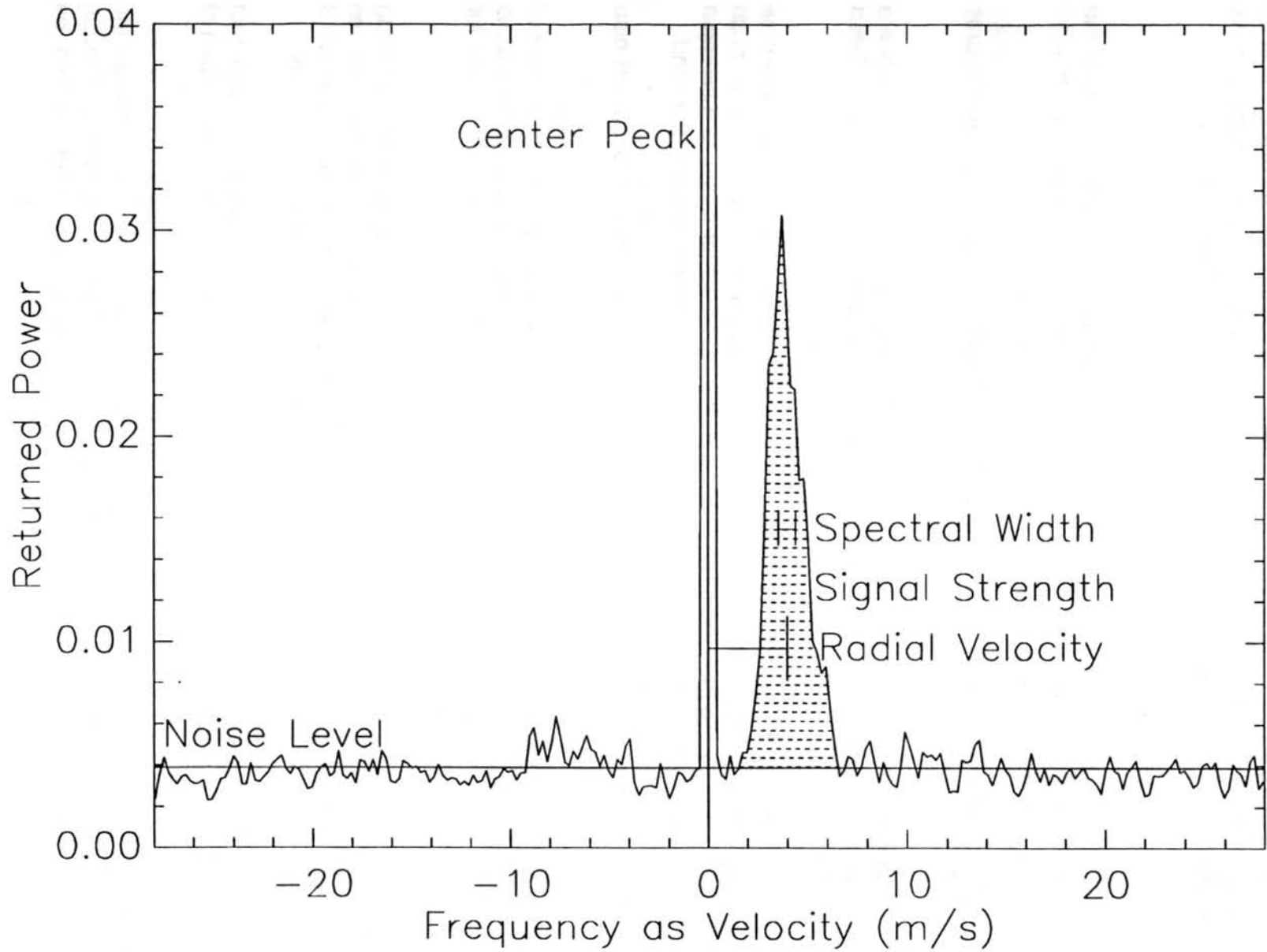


Figure 2. A typical wind profiler doppler spectrum.

1.3 Limitations

Unfortunately the radial velocities derived from wind profiler spectra are sometimes spurious. This is due to hardware limitations and to assumptions inherent in the processing of the wind profiler measurements. These assumptions include:

- 1) The wind profiler measures only air motion;
- 2) Air motions are uniform over the distance between the beams and over the time period required for the wind profiler to cycle through all its beams (10 minutes normally for the CSU wind profiler); and
- 3) Precipitation falls uniformly and steady through all the wind profiler beams for the single cycle time period.

Because of these assumptions and other hardware limitations spurious winds are sometimes reported. Some sources of spurious wind measurements are listed below.

- 1) Returns from side lobe emissions can overwhelm the true signal when the return comes from a hard target. (A hard target is an object that is much more dense than air.) The ground clutter of the center peak is an example of this, and may represent vegetation on a hill side moving in the wind.
- 2) Spurious targets in the path of the beam, like airplanes or birds, will also overwhelm the true signal return from the air.
- 3) Precipitation fall velocities can dominate the vertical velocity component of the signal, and will contaminate the horizontal winds if the precipitation does not fall at a uniform and steady rate through all the wind profiler beams for the entire single cycle time period.
- 4) As the wind profiler switches from transmitting the radar pulses to receiving the return signal, there is some electronic noise in the system that requires a few microseconds to dissipate. This receiver recovery noise can affect the lowest gates if enough time is not given for the system to recover.
- 5) Spurious winds can result from horizontal and vertical wind fields that change during the single cycle time period or vary over the spacial span of the wind profiler beams.
- 6) Stationary waves, such as those created in a lee of a mountain, causes the vertical velocity to vary spatially with distance from the mountain. Though the vertical velocities may be quite constant, each beam could be measuring a different vertical velocity.

- 7) If the measured velocity exceeds the maximum (or minimum) radial velocity then velocity folding occurs. The velocity is folded back in as a value near the minimum (or maximum) possible value. It is similar to a speedometer dial where the needle travels more than 360 degrees to measure very fast speed.

2.0 Quality Control Methods

Four wind profiler quality control methods will be reviewed: consensus averaging based on work of Fischler and Bolles (1981); the method developed by the National Oceanic and Atmospheric Administration (NOAA) for its wind profiler demonstration network (Brewster and Schlatter, 1988; Brewster, 1989); the continuity method of Weber and Wuertz (1991; Weber, *et al*, 1993); and the method developed at CSU (Hein, *et al*, 1991).

2.1 Consensus Averaging

Consensus averaging consists of averaging a subset of similar valued data points together. Points that differ significantly from the majority are not included in the average. There is a minimum number of points required to form a consensus average. Consensus averaging is commonly used to make hourly averages and usually has been used in conjunction with the other methods. Consensus averaging assumes only gradual wind shifts in either or both space and time.

2.2 NOAA Network Method

The NOAA network method makes use of shear in wind speed and in wind direction to identify spurious points in the u and v components of the wind. It first removes extreme values by using a threshold and the median of 8 neighboring points. The 8 neighboring points are the 2 surrounding points in height and the 6 points from the previous 2 time periods at the height of the point in question and the points above and below that height. The shears calculated from the wind speed and wind direction are used to determine the threshold value. A point interpolated between the points above and below the point in question is compared with the point in question using the threshold to determine the validity of this point. This method is used in real time by the NOAA Demonstration Network in conjunction with the consensus method.

2.3 Continuity Method

The continuity method of Weber and Wuertz makes use of pattern matching techniques and continuity to separate out the spurious radial velocities. First the data are built into patterns making use of a threshold to help determine continuity. The individual points are then compared with an interpolated value from its neighborhood in the pattern and its validity is determined. Any small patterns remaining are eliminated, leaving the large patterns to form the dataset. The continuity method has the advantage of processing profiles where the opposing beams and the high and low modes are combined into a single profile. This

creates a profile with double the number of points and some overlap between high and low modes. The combined profile allows for better continuity. With the combined profile, if the two opposing beam velocities disagree the correct velocity component based on continuity can be chosen. This method was used to process the combined profiles of u and v for the CSU Wind Profiler FIRE and ASTEX data sets (Cox, *et al*, 1992; Cox, *et al*, 1993).

2.4 CSU Method

To find spurious points the CSU method makes use of the return signal moments: the signal strength, radial velocity, and spectral variance (spectral width of the peak). The data point is checked for a narrow spectral width and for a signal strength that is significantly different from the other beams' signal strengths. If one of these conditions is violated the data point is considered spurious. A data point that passes the first set of criteria is then compared with its surrounding neighbors and if its radial velocity is significantly different from its neighbors' radial velocities, it too is considered a spurious point. Because of the signal strength check, the CSU method has performed well in identifying data points caused by ground clutter or other hard targets. The check for a narrow spectral width, employed in the CSU method enables identification of points caused by system noise.

3.0 Beam comparison

The relative accuracy of the horizontal wind measurements can be determined by comparing the velocities from the off-vertical beam to those from its opposing beam counterpart. Differences between the velocities provide a measure of instrument capability under the limiting assumptions. Data from 12 November to 7 December 1991 from the FIRE II Cirrus IFO site at Parsons, Kansas (Cox, *et al*; 1992) were used to evaluate the wind profiler. A quality control method was used to filter the data before comparison. By making use of several quality control methods, a comparison of methods was possible.

3.1 Background

The radial velocities of each of the five beams for a given height can be expressed as:

$$\begin{aligned}
 V_{rn} &= -(v + \delta v_n) \sin\theta - (w + \delta w) \cos\theta \\
 V_{re} &= -(u + \delta u_e) \sin\theta - (w + \delta w) \cos\theta \\
 V_{rs} &= +(v + \delta v_s) \sin\theta - (w + \delta w) \cos\theta \\
 V_{rw} &= +(u + \delta u_w) \sin\theta - (w + \delta w) \cos\theta \\
 V_{rz} &= -(w + \delta w)
 \end{aligned}$$

where the radial velocities (V_r) are positive toward the wind profiler and the subscripts n , s , e and w denote north, south, east and west. u is the true mean east-component of the wind and v is the true mean north-component. w is the true mean vertical velocity which contains the vertical wind and/or the vertical

motion of hydrometers. θ is the angle off vertical of the beams (15°). The error terms (δ) contain instrument measurement errors as well as errors due to spatial and temporal variations in the wind field.

There are two independent measurements of u and v by the opposing beams. These measurements can be compared by differencing the horizontal wind components.

$$\begin{aligned}\Delta u &= u_w - u_e = \delta u_w - \delta u_e = (V_{re} + V_{rw} + 2(W + \delta W) \cos\theta) / \sin\theta \\ \Delta v &= v_s - v_n = \delta v_s - \delta v_n = (V_{rn} + V_{rs} + 2(W + \delta W) \cos\theta) / \sin\theta\end{aligned}$$

In the above difference equations, the vertical velocity contributes equally to both equations. The effect of the vertical velocity can be isolated by a coordinate transformation of Δu and Δv (Strauch, *et al*; 1987). The Δu and Δv coordinates are rotated 45° to produce the ΔC and ΔS coordinates. The resulting equations are:

$$\begin{aligned}\Delta C &= (\Delta v + \Delta u) / 2^{1/2} = (\delta v_s - \delta v_n + \delta u_w - \delta u_e) / 2^{1/2} \\ &= (V_{rn} + V_{rs} + V_{re} + V_{rw} + 4(W + \delta W) \cos\theta) / \sin\theta / 2^{1/2}\end{aligned}$$

$$\begin{aligned}\Delta S &= (\Delta v - \Delta u) / 2^{1/2} = (\delta v_s - \delta v_n - \delta u_w + \delta u_e) / 2^{1/2} \\ &= (V_{rn} + V_{rs} - V_{re} - V_{rw}) / \sin\theta / 2^{1/2}\end{aligned}$$

Figure 3 displays wind profiler data in Δu and Δv coordinates with the ΔC and ΔS axes also displayed. Note the effect of the vertical velocity as the points stretch out along the ΔC axis. Since ΔS is unaffected by the vertical velocity component, it will be used to compare the opposing beams.

3.2 Comparison of the Measurements and the Quality Control Methods

Three time periods from the FIRE II data set were used so that the variability over time can also be explored. The data from the time periods were first filtered by a quality control method (one of three) and then the remaining "good" data, where radial velocities from all four off-vertical beams were available, were used to calculate Δu , Δv and ΔS .

In Figures 4-6, the fraction of "good" points, the mean difference (the mean of Δu , Δv or ΔS), its standard deviation and its adjusted absolute deviation¹ are

¹Absolute deviation ($\sigma_{AD} = \sum |X - \bar{X}| / N$) for a normal distribution is 0.8 times the size of the standard deviation. The absolute deviation is less affected by outliers than the standard deviation. In the figures of this report, the absolute deviation has been adjusted to be used as a robust estimation of the standard deviation.

FIRE II Parsons, KS: Nov 10-19, 1991 Continuity Method

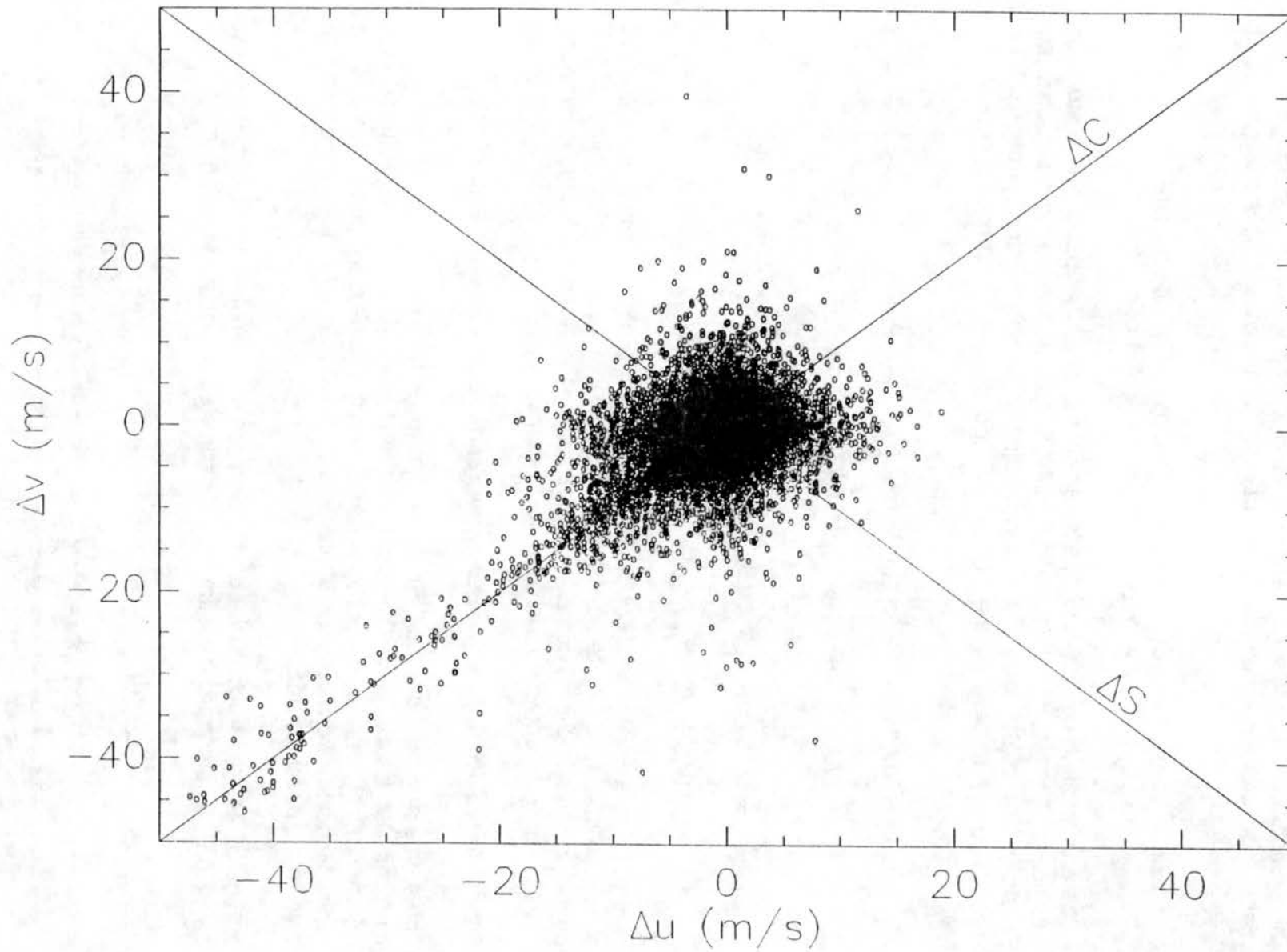


Figure 3. The variability of wind profiler data is seen. Note how the effect of the vertical velocity can be removed by using ΔS .

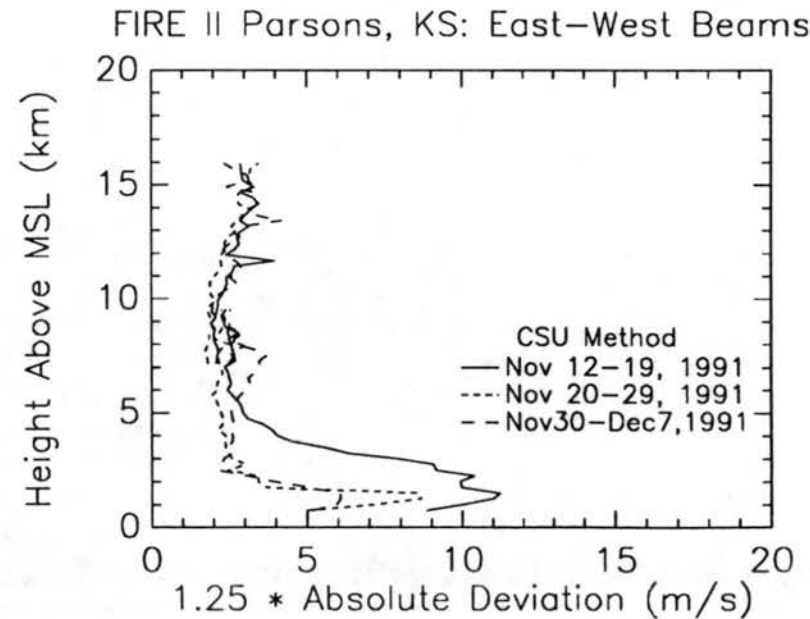
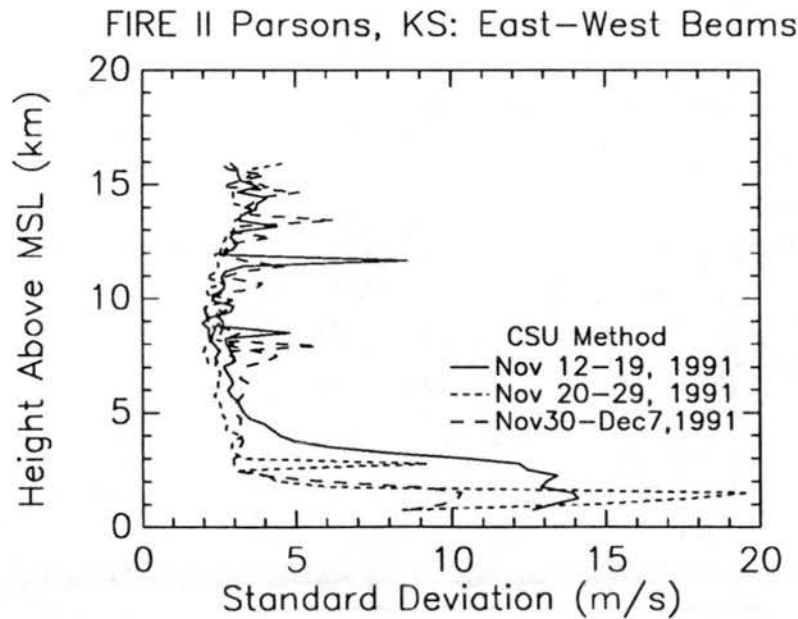
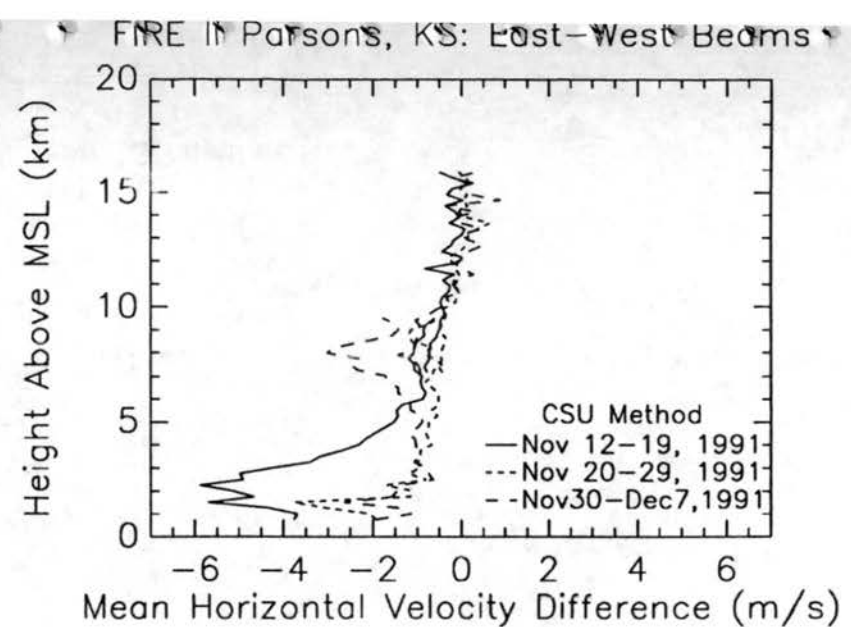
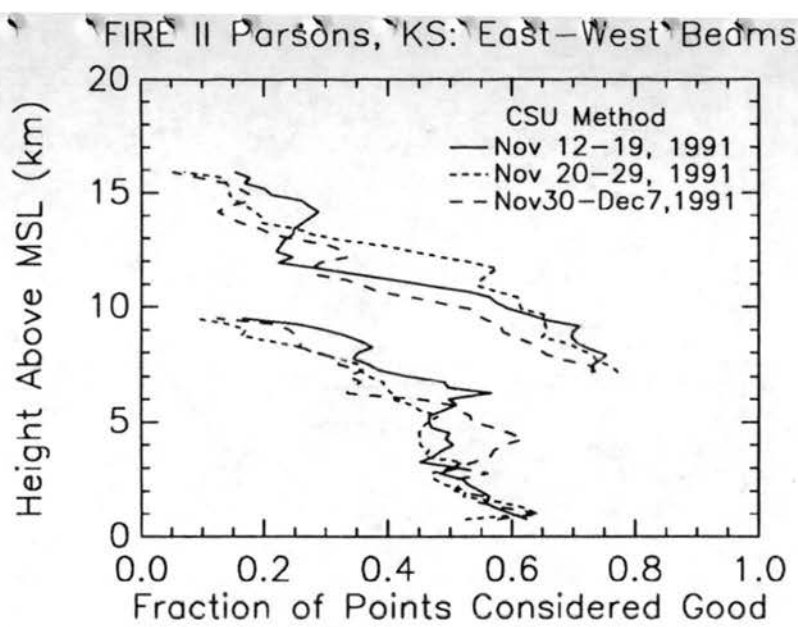


Figure 4. A comparison of the east and west beams using the CSU method.

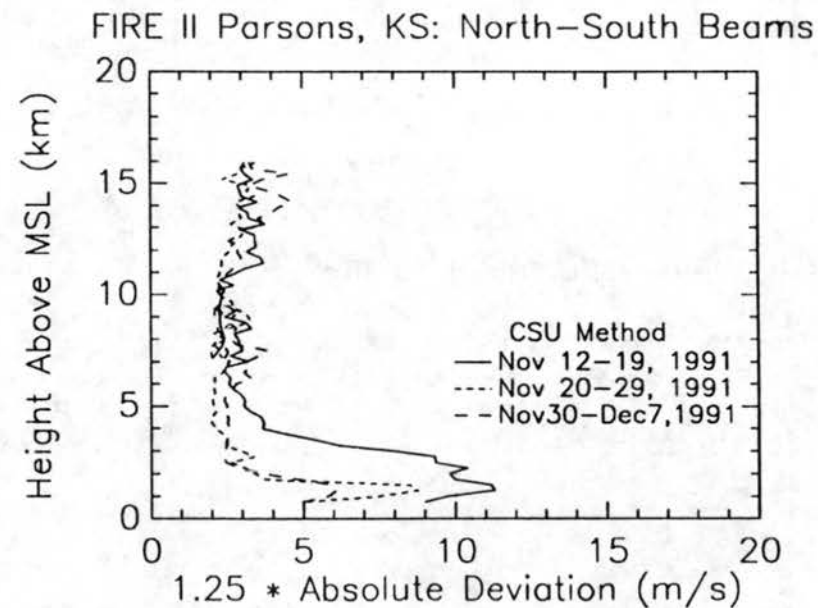
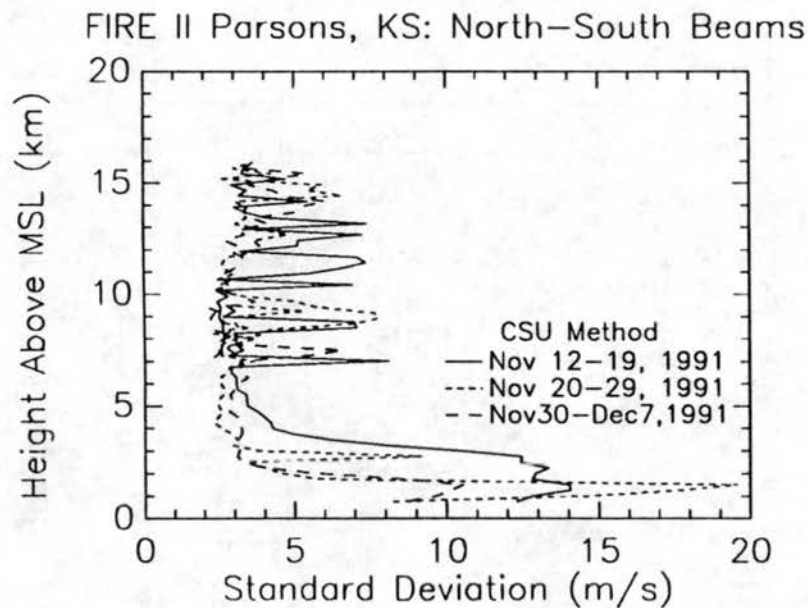
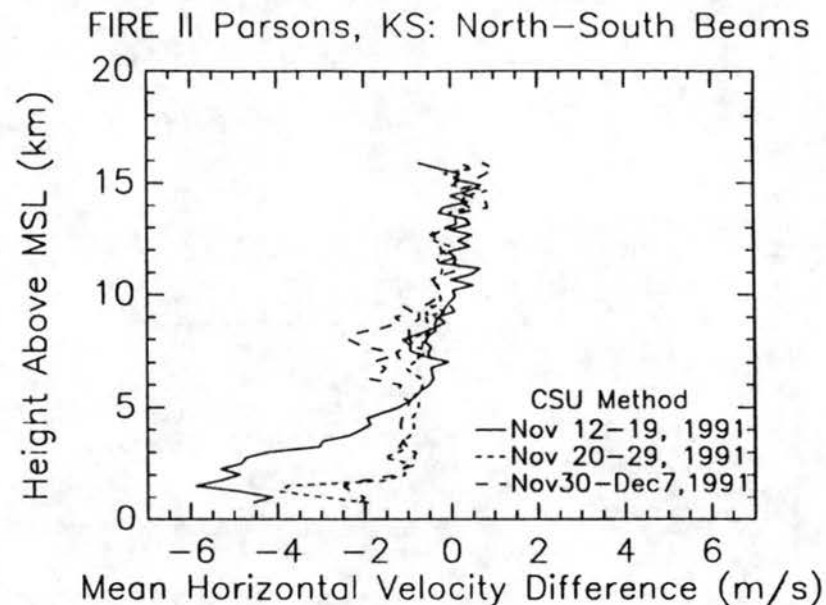
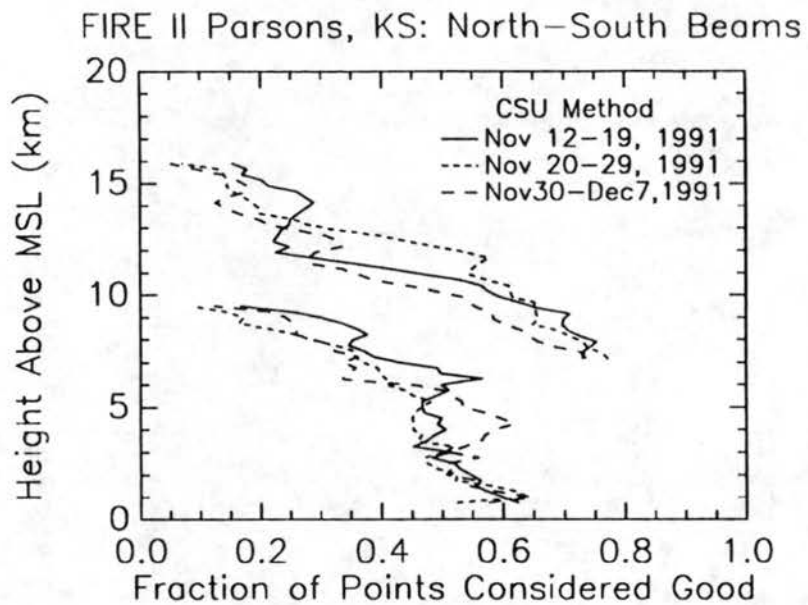


Figure 5. A comparison of the north and south beams using the CSU method.

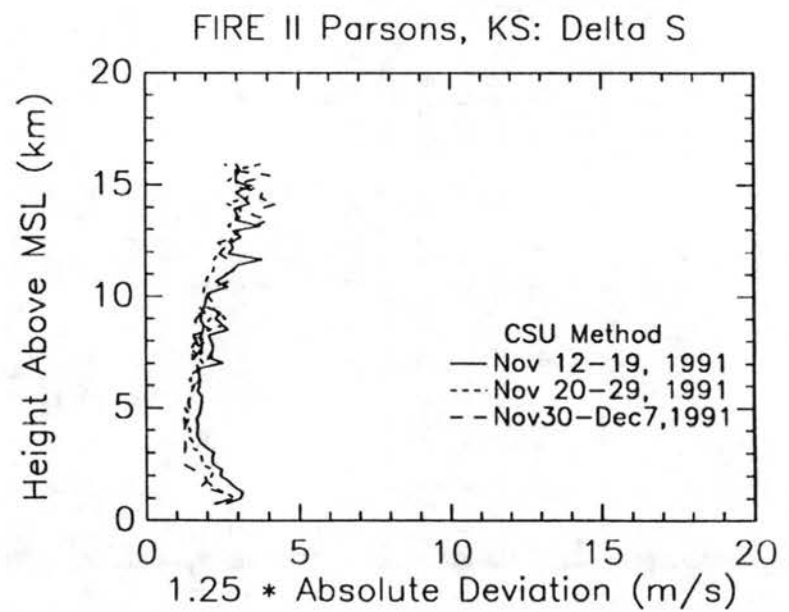
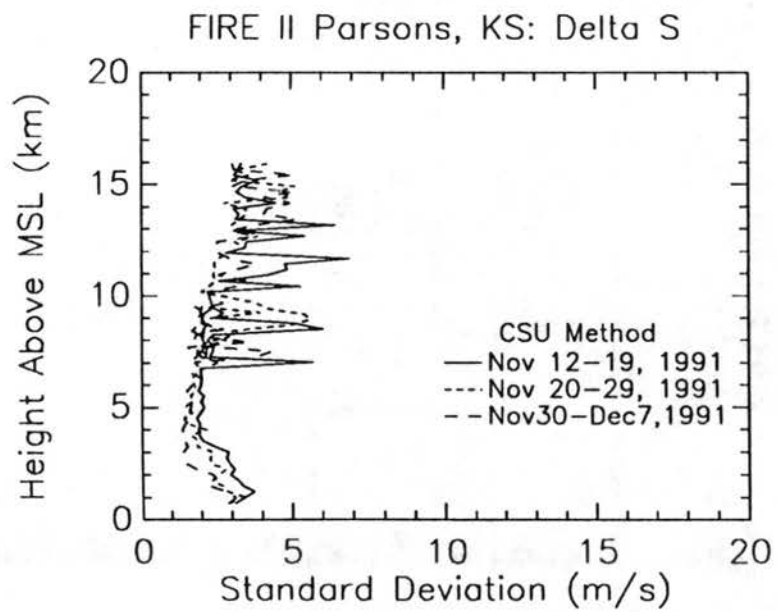
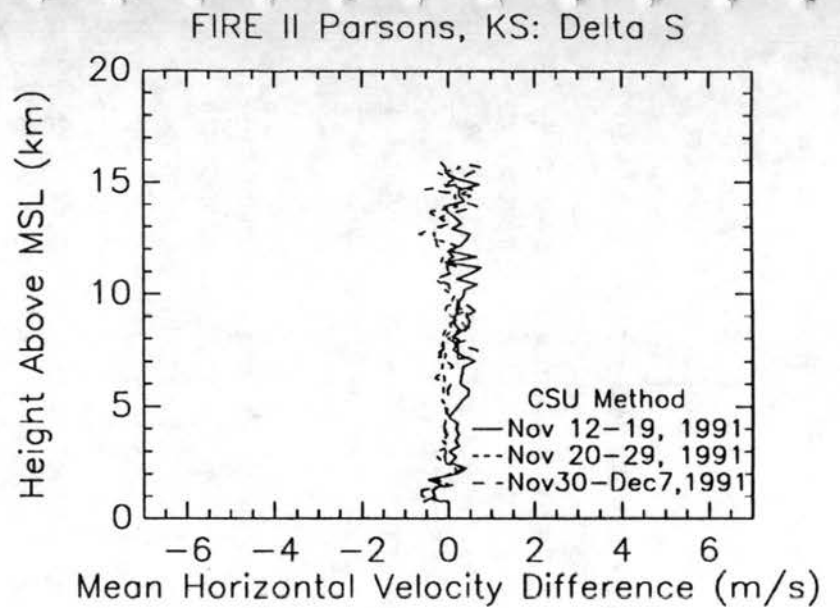
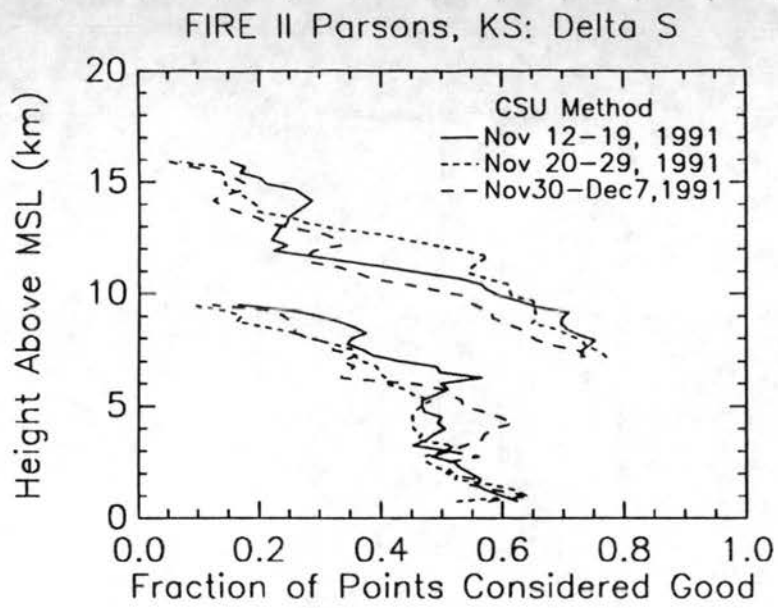


Figure 6. A comparison of beams using the CSU method: ΔS .

displayed with height for data filtered with the CSU method. Results very similar to the results from the data processed by the CSU method are shown for the NOAA network method (Figures 7-9) and for the continuity method (Figures 10-12). At the higher altitudes one sees fewer points and a larger standard deviation. This arises from the weak (and therefore noisy) return signal, which allows for many spurious measurements. The adjusted absolute deviation (a robust estimate of the standard deviation) is less affected by the remaining spurious points. The mean values tend to be close to zero indicating that there is not a bias of one beam over another, however the mean values of Δu and Δv are significantly different than zero near the ground (at heights 1-3 km). This is likely due to a side lobe reflection of some ground feature. Noting that the results from the three time periods are quite similar suggests that the time periods were long enough to produce reliable averages and that reliable conclusions may be drawn from these results.

One can compare how the results vary among the methods and determine the best method for the data set. Tables 2-4 display the mean of ΔS , its standard deviation and the percentage of points accepted as reliable by the three methods. The premise applied is that the smaller the mean and standard deviation and the larger the percentage of "good" points the better the method performed. This assumes that bad points contribute to a bias and a large standard deviation and also that the method which removes the largest number of bad points while eliminating the smallest number of good points is superior. From Tables 2-4 it is apparent that the continuity method out-performed the other two methods (by smaller means and standard deviations, and by a larger percentage of points marked as good). Because of these results, the continuity method was chosen to process the CSU wind profiler FIRE and ASTEX data sets.

Table 2.

Mean ΔS (m/s)			
Time Period	CSU	NOAA Network	Continuity
Nov 12-19, 1991	0.201	0.198	0.177
Nov 20-29, 1991	-0.078	-0.049	-0.041
Nov 30 - Dec 7, 1991	0.007	0.032	-0.004

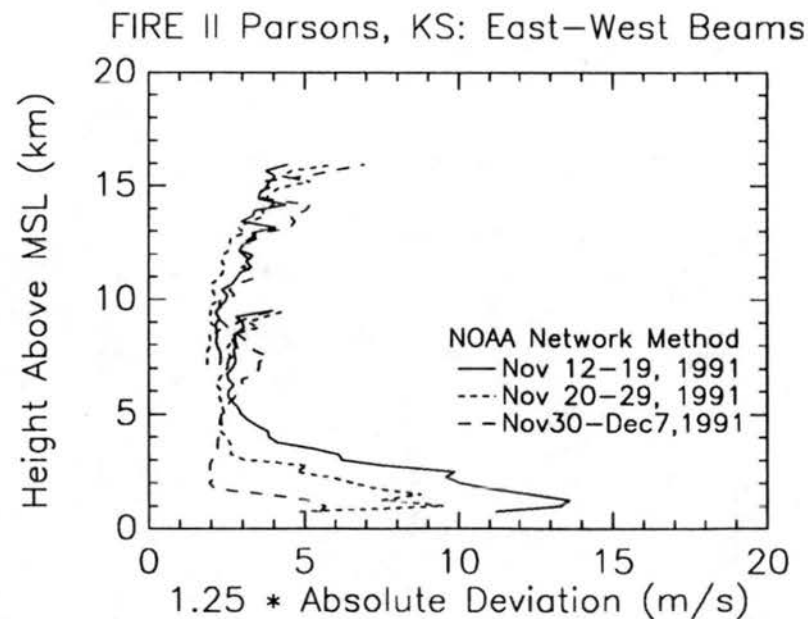
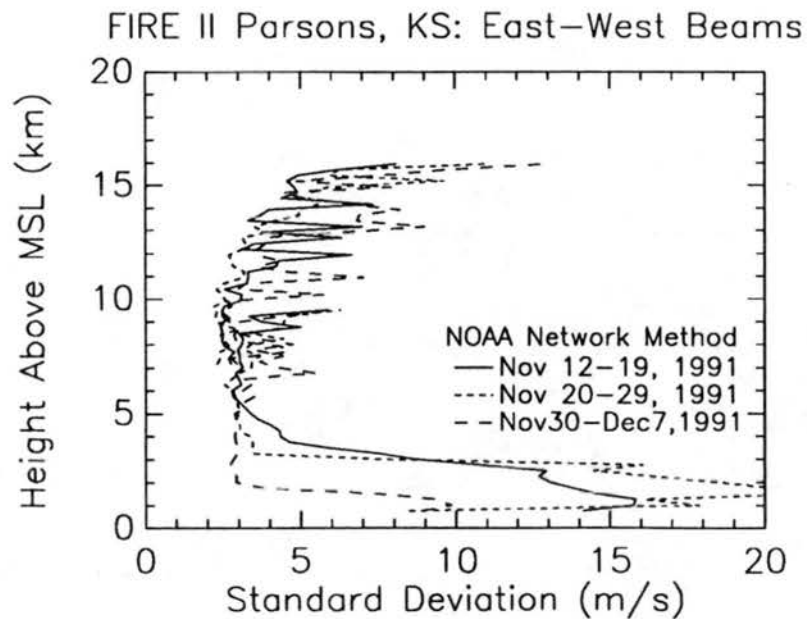
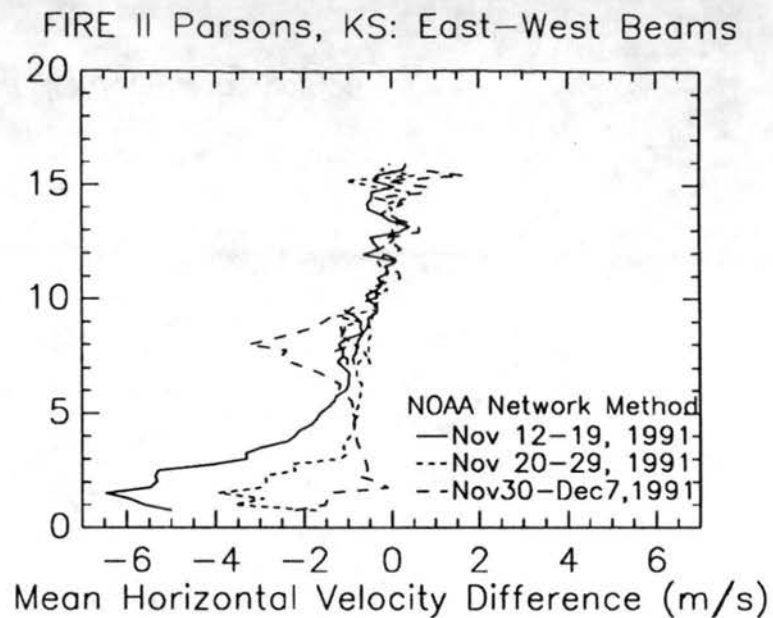
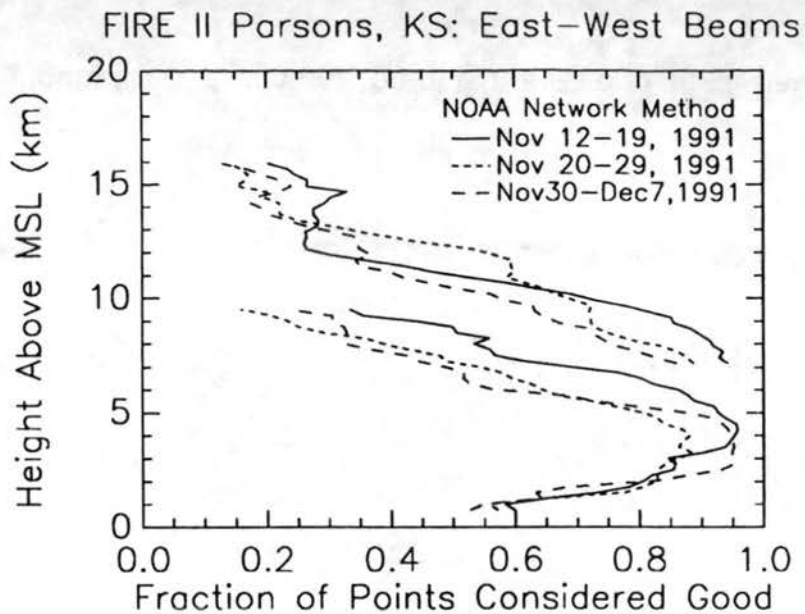


Figure 7. A comparison of the east and west beams using the NOAA network method.

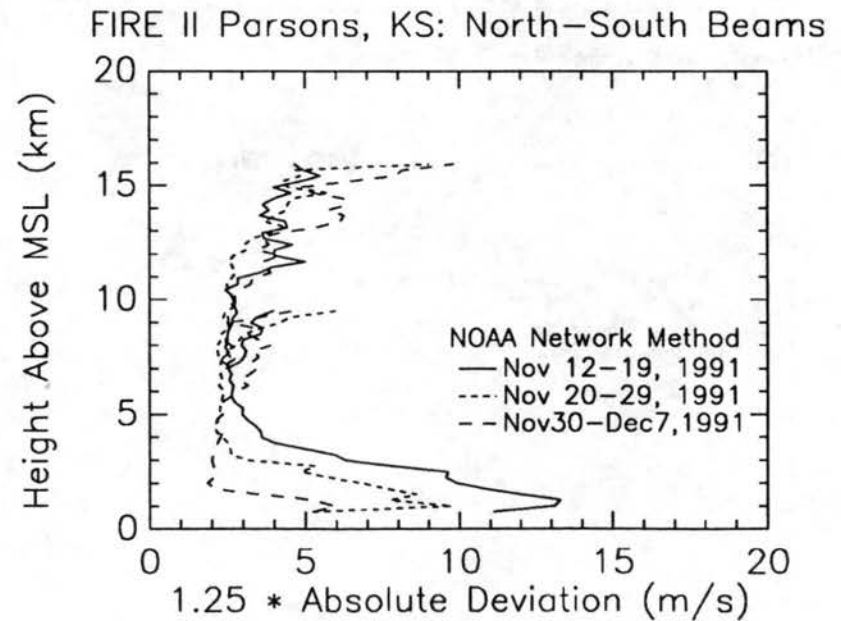
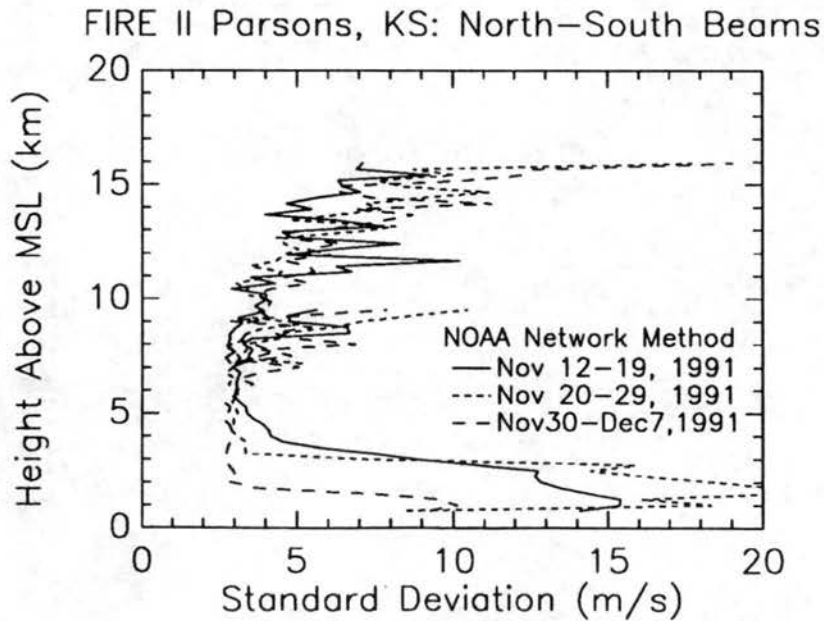
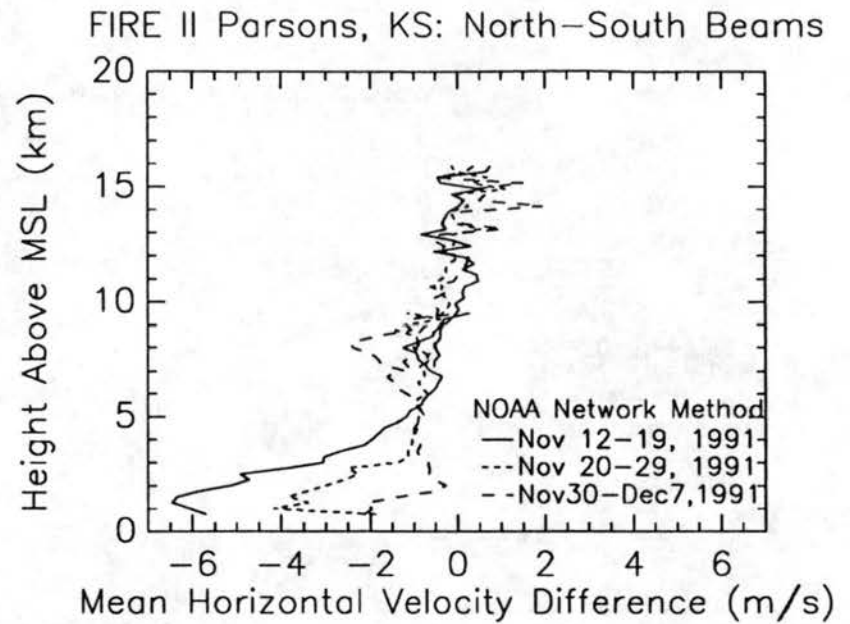
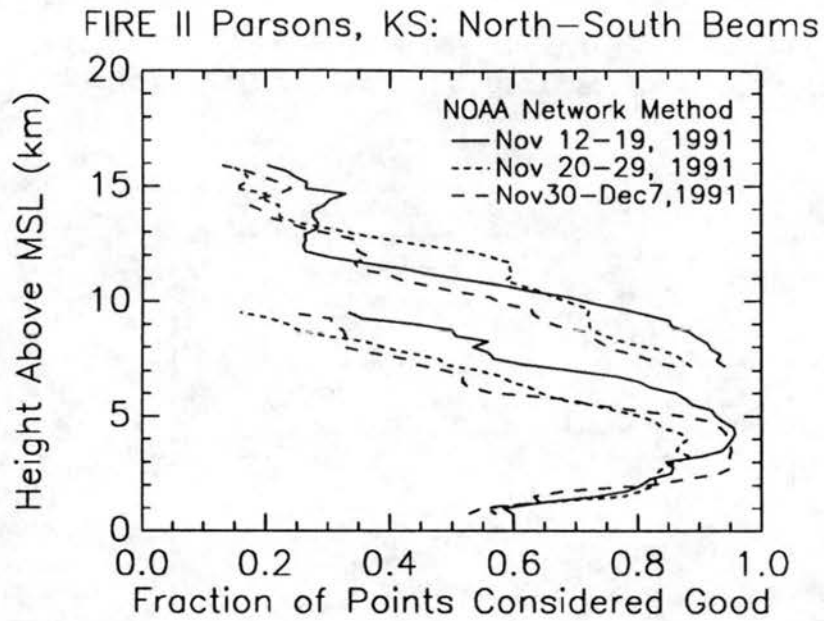


Figure 8. A comparison of the north and south beams using the NOAA network method.

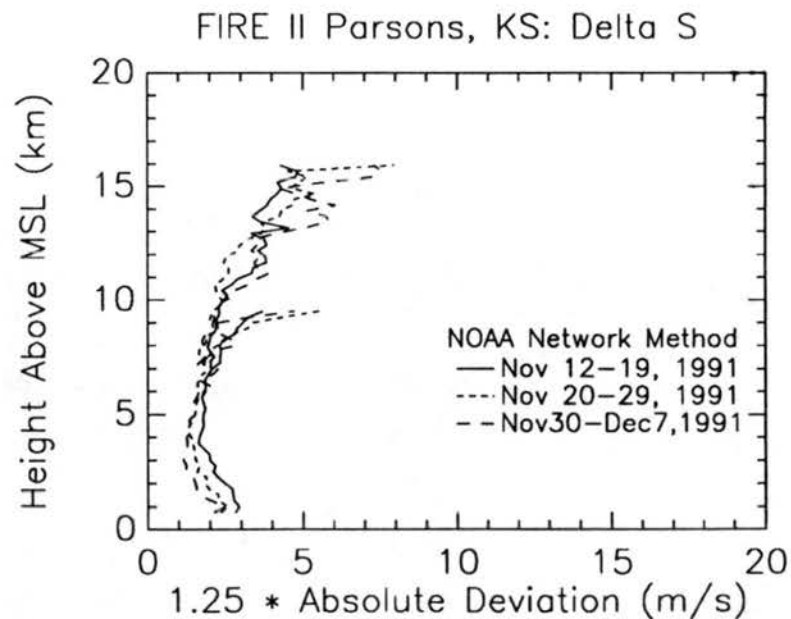
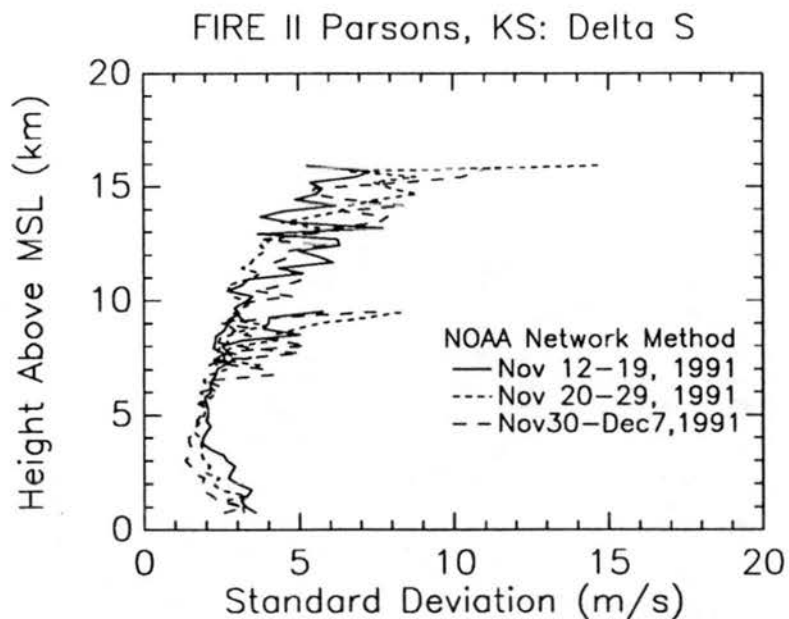
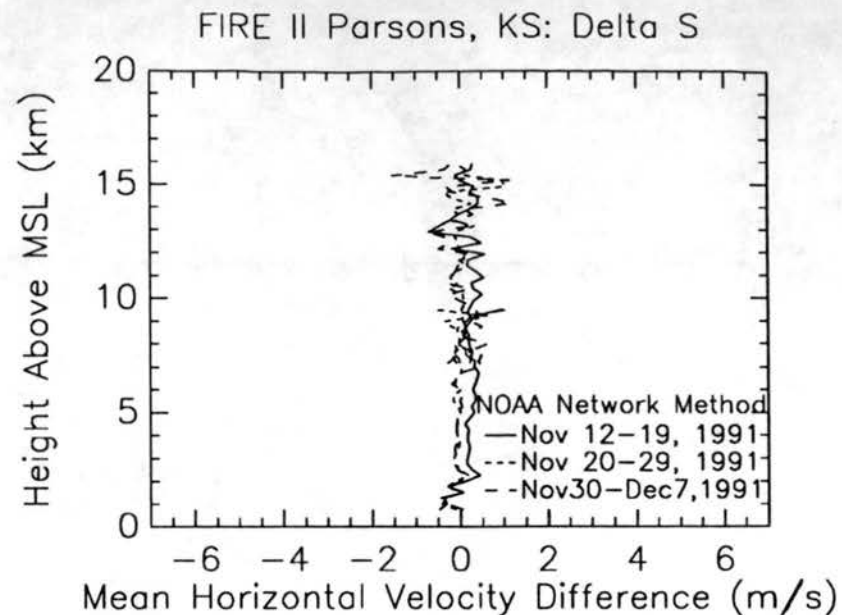
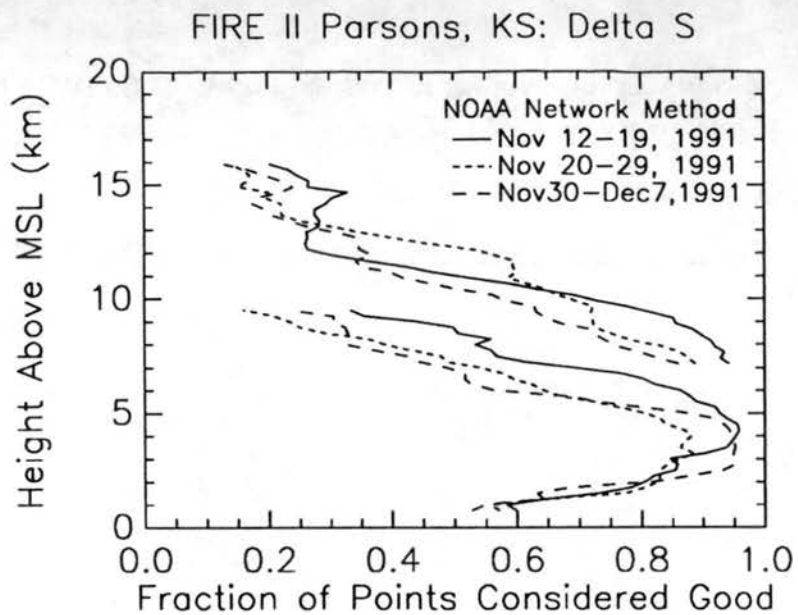


Figure 9. A comparison of beams using the NOAA network method: ΔS .

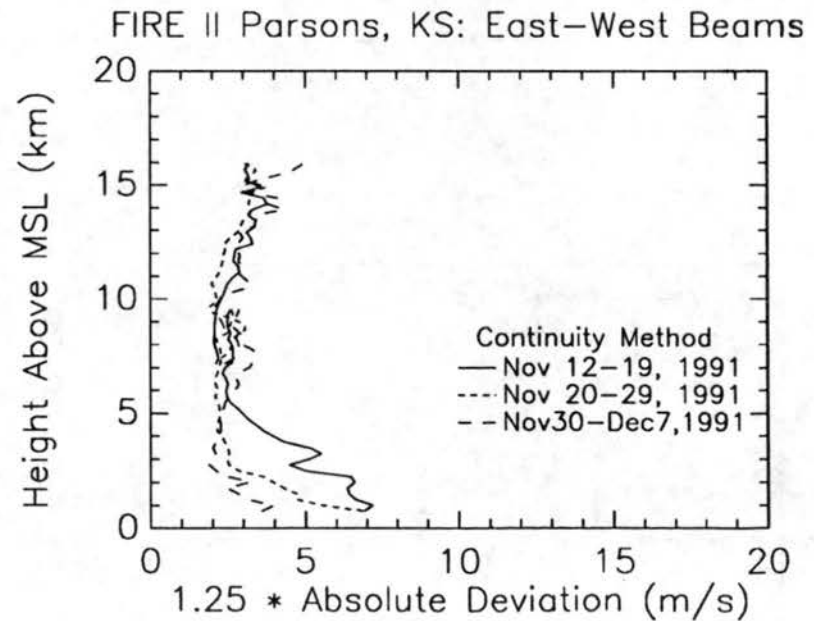
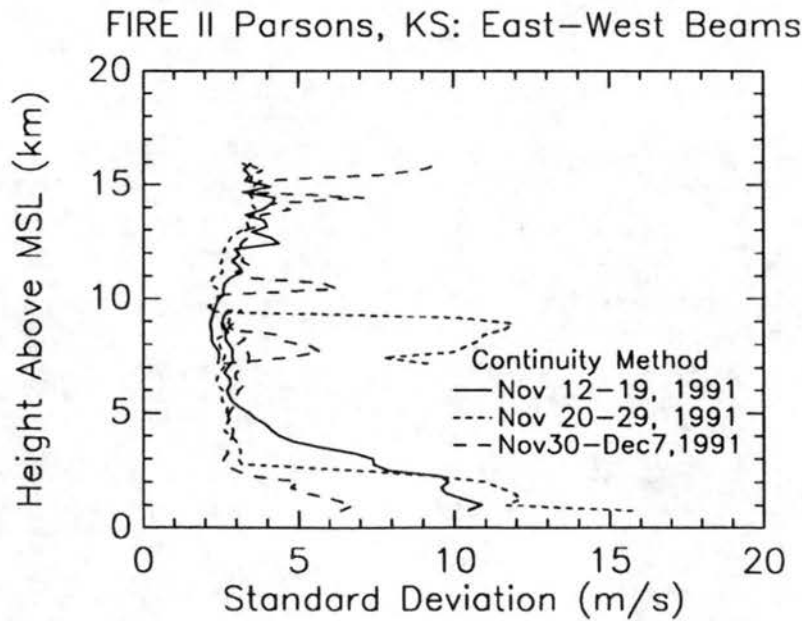
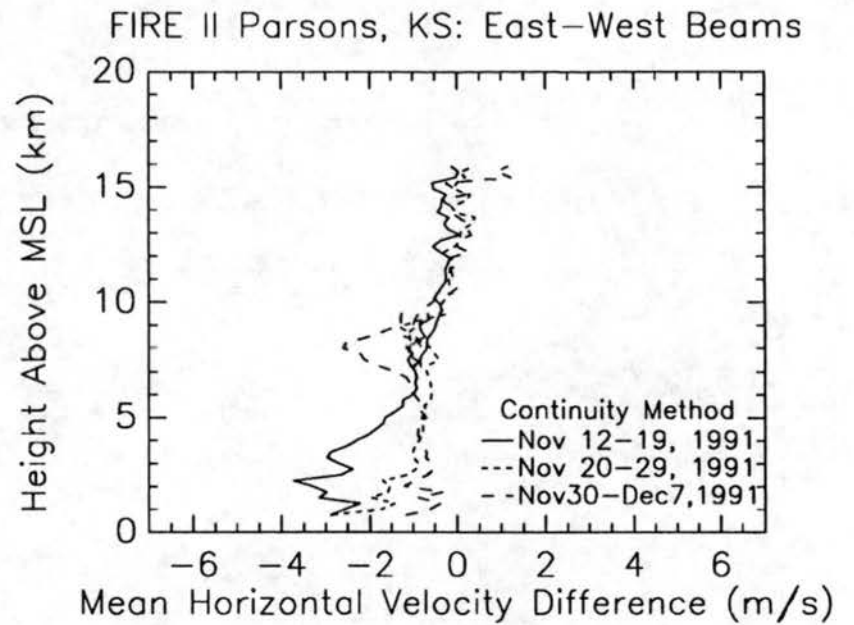
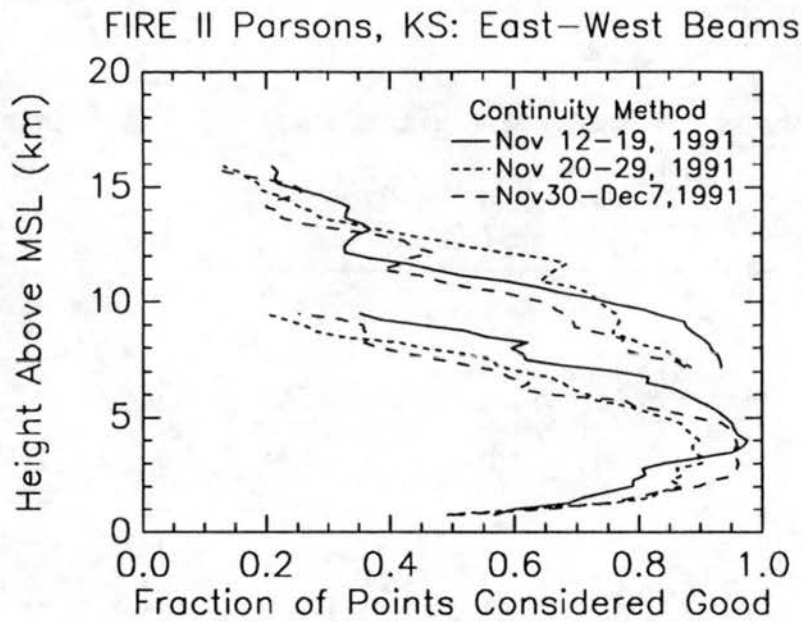


Figure 10. A comparison of the east and west beams using the continuity method.

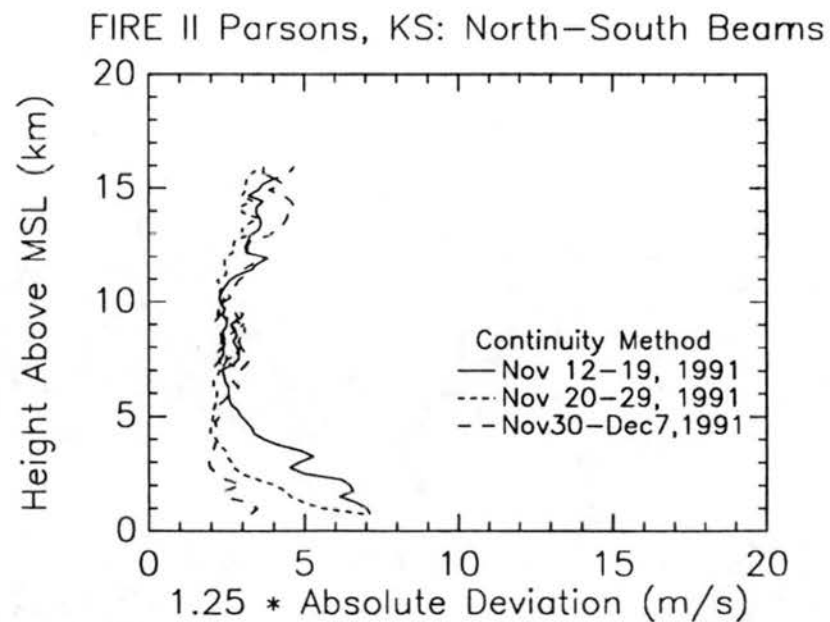
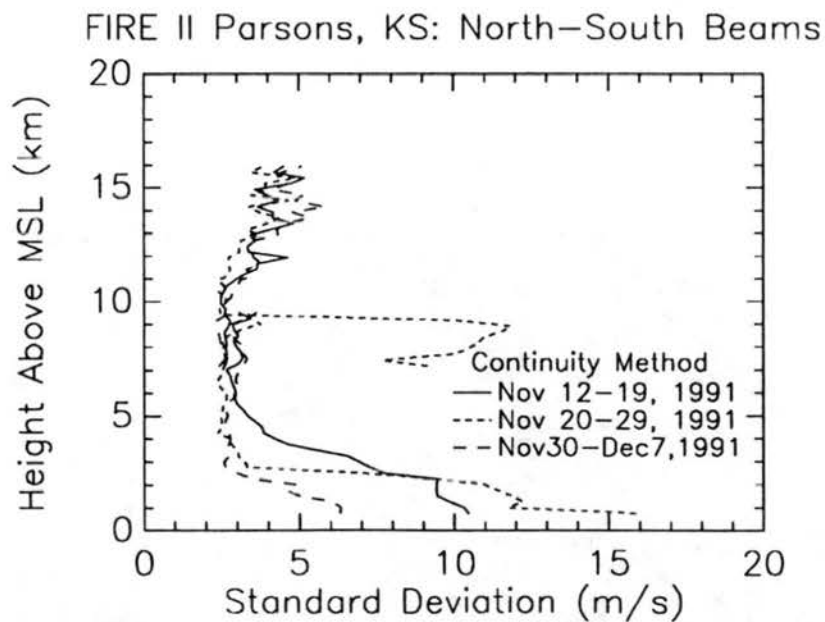
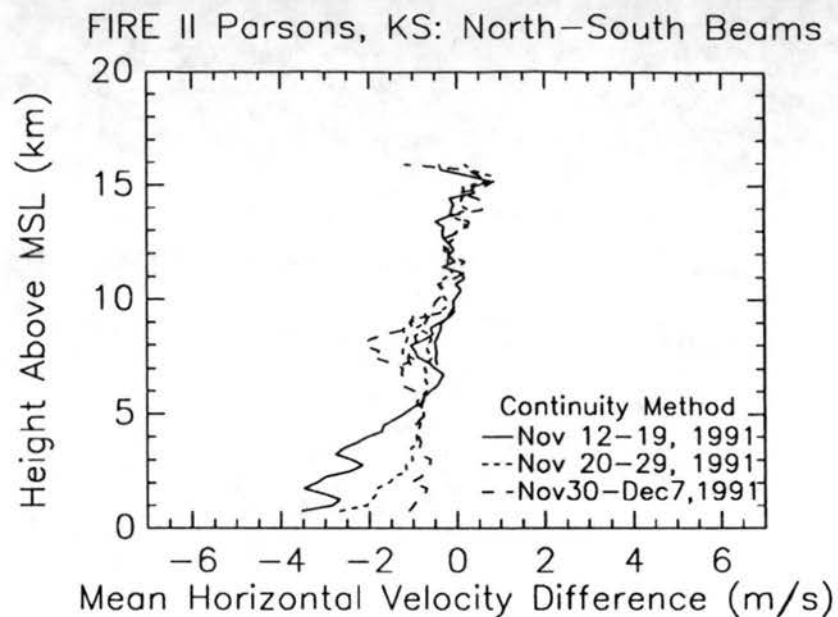
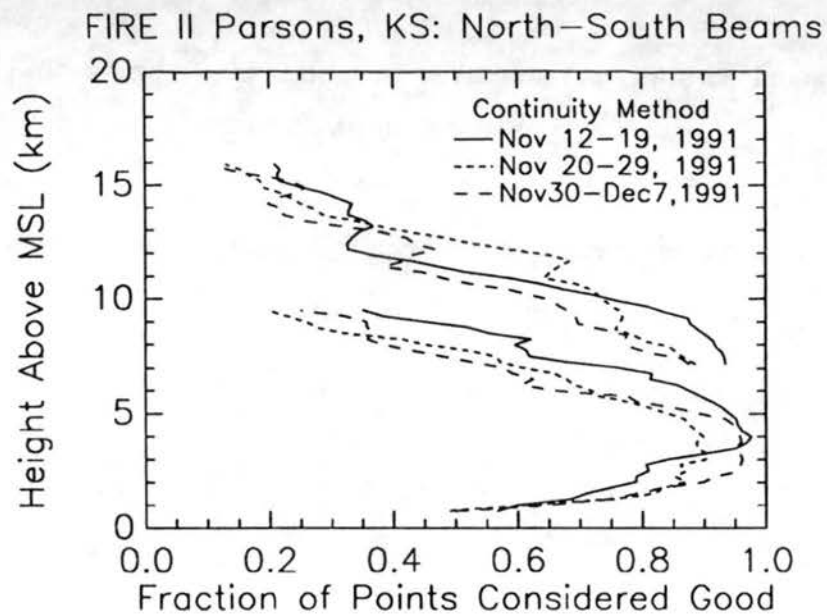


Figure 11. A comparison of the north and south beams using the continuity method.

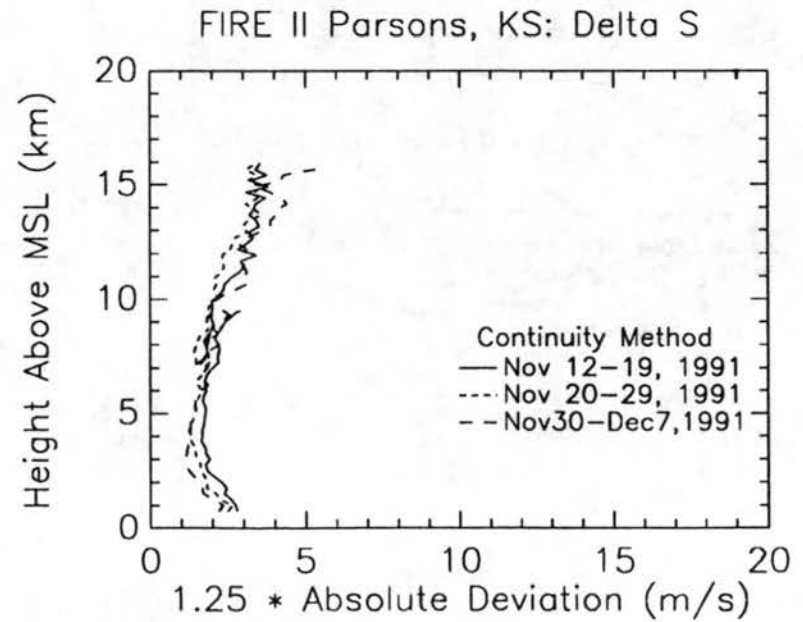
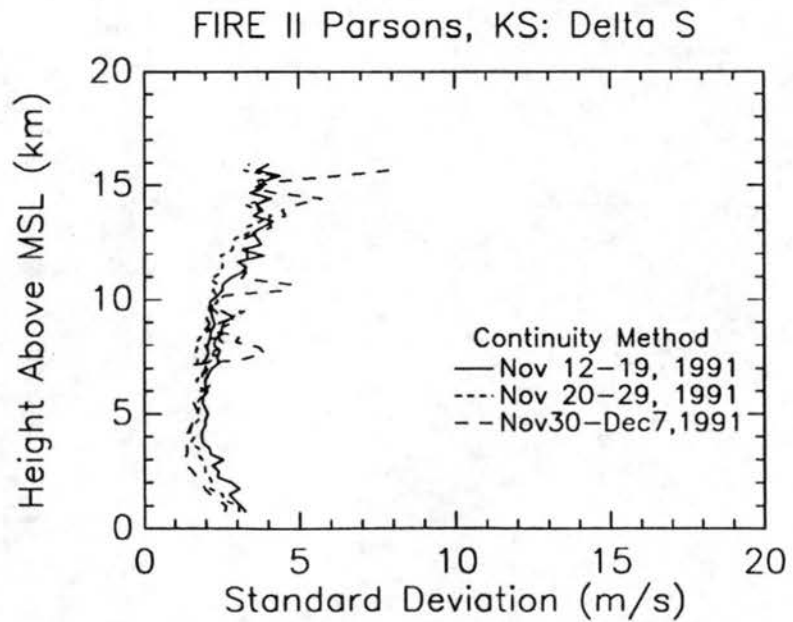
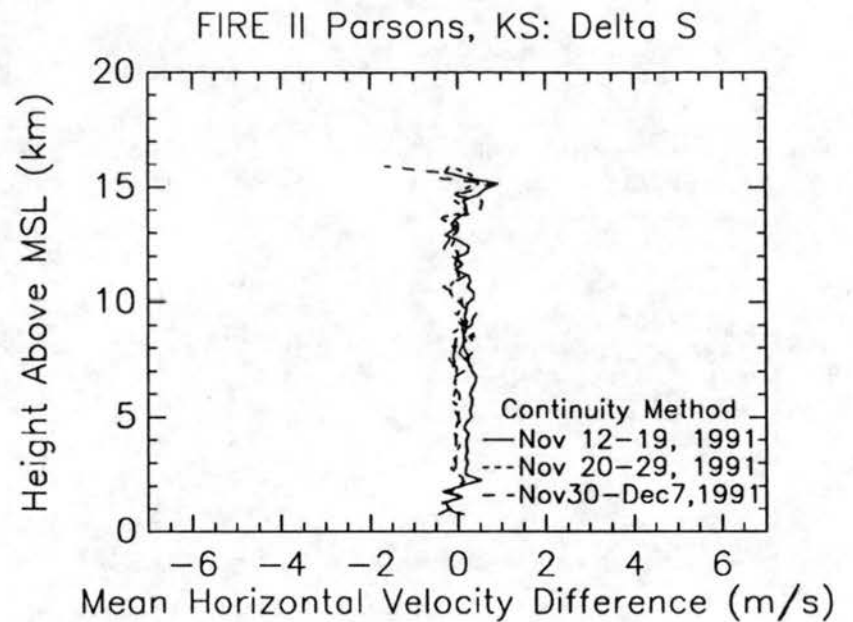
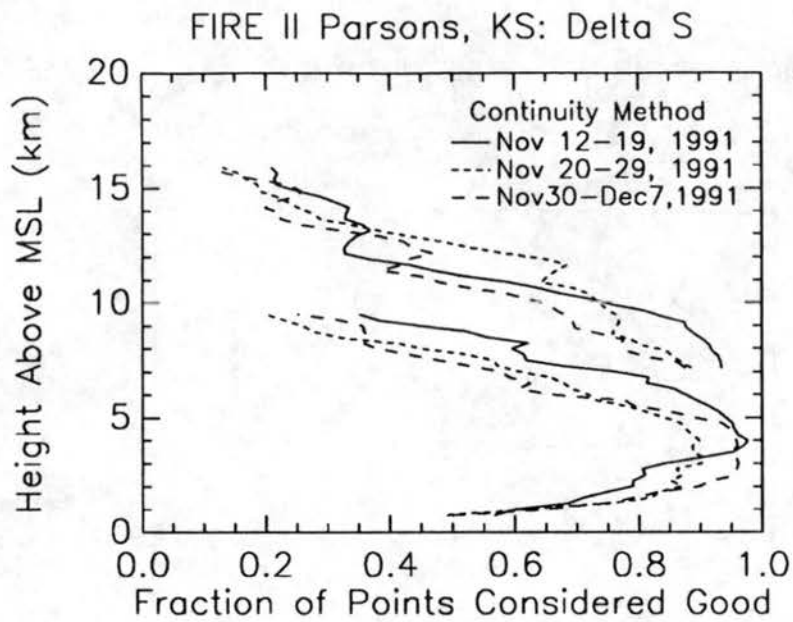


Figure 12. A comparison of beams using the continuity method: ΔS .

Table 3.

ΔS Standard Deviation (m/s)			
Time Period	CSU	NOAA Network	Continuity
Nov 12-19, 1991	3.030	3.242	2.519
Nov 20-29, 1991	2.890	3.340	2.261
Nov 30 - Dec 7, 1991	2.470	3.487	2.630

Table 4.

Percentage of Data where All 4 Beams were Marked as "Good"			
Time Period	CSU	NOAA Network	Continuity
Nov 12-19, 1991	44.5	63.0	65.2
Nov 20-29, 1991	43.5	57.2	61.5
Nov 30 - Dec 7, 1991	40.9	54.2	58.7

3.3 Comparison with the Porto Santo Data Set

The question may be posed: "How representative are the results from Parsons, KS?" Similar processing for the ASTEX data set collected on Porto Santo Island (Cox, *et al*, 1993) was performed using the CSU method. Results shown in Figures 13-15 and in Table 5 indicate similar findings for the ASTEX data as was reported above for the FIRE data though the magnitudes are smaller. The mean values of Δu and Δv did not have their maxima near the ground, rather it was at 2.5 to 3 km, which corresponds well to the hills on the island which were 2-3 km from the wind profiler. In this case the mean value of ΔS also varied significantly from zero at about the 2.5 km height. The reason for the smaller magnitudes is likely due to the large fraction of the data that was removed from consideration by the CSU method.

Table 5.

Porto Santo (ASTEX): CSU Method			
Time Period	Mean ΔS (m/s)	ΔS Standard Deviation	Percentage of "Good" Data
June 10-19, 1992	-0.054	2.097	28.4
June 20-28, 1992	-0.024	2.073	20.4

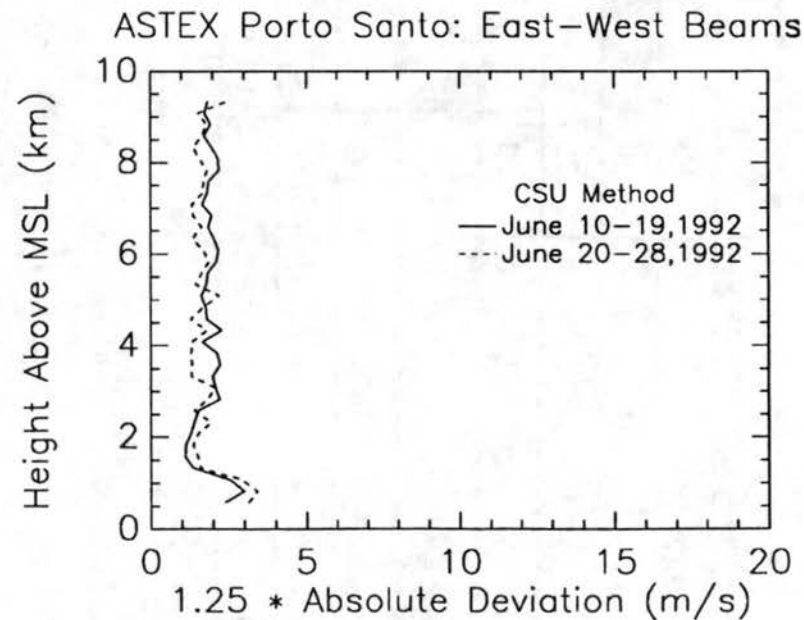
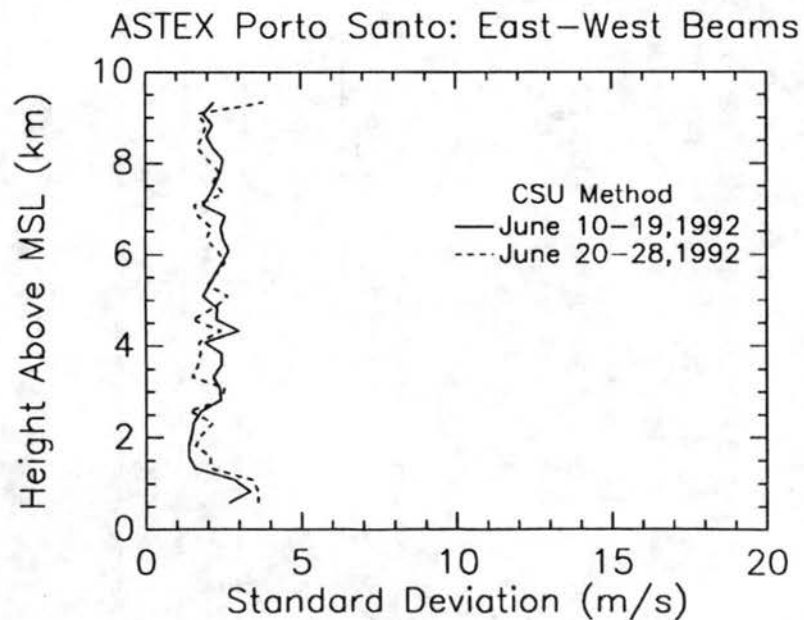
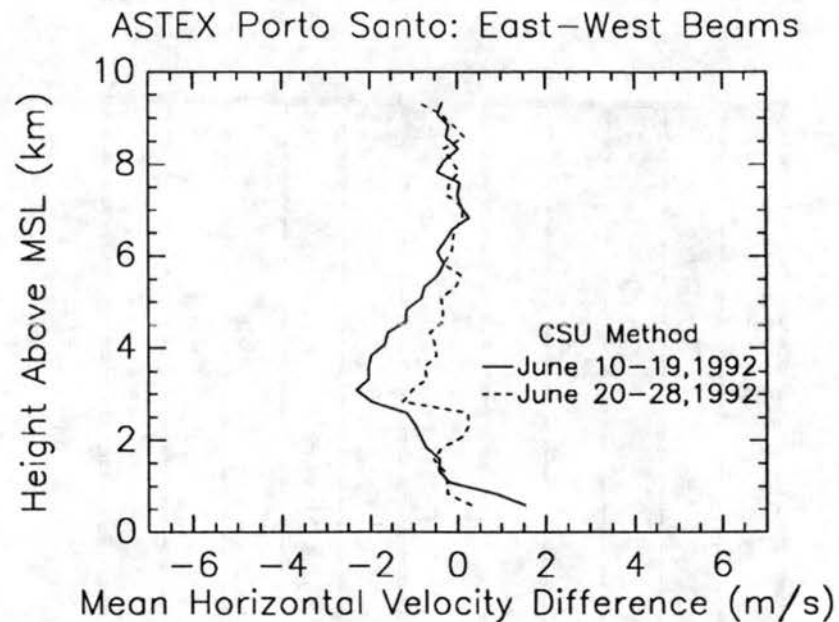
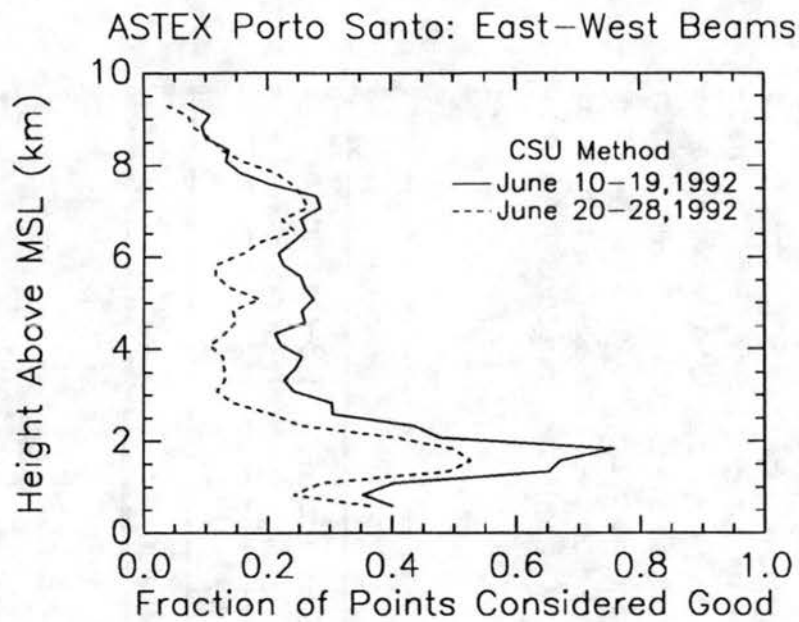


Figure 13. A comparison of the east and west beams using the CSU method on data from Porto Santo.

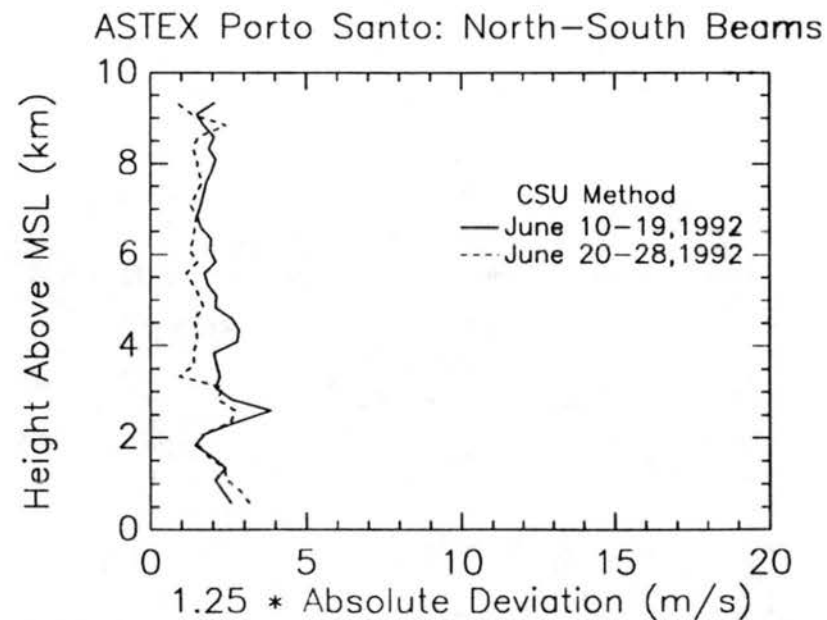
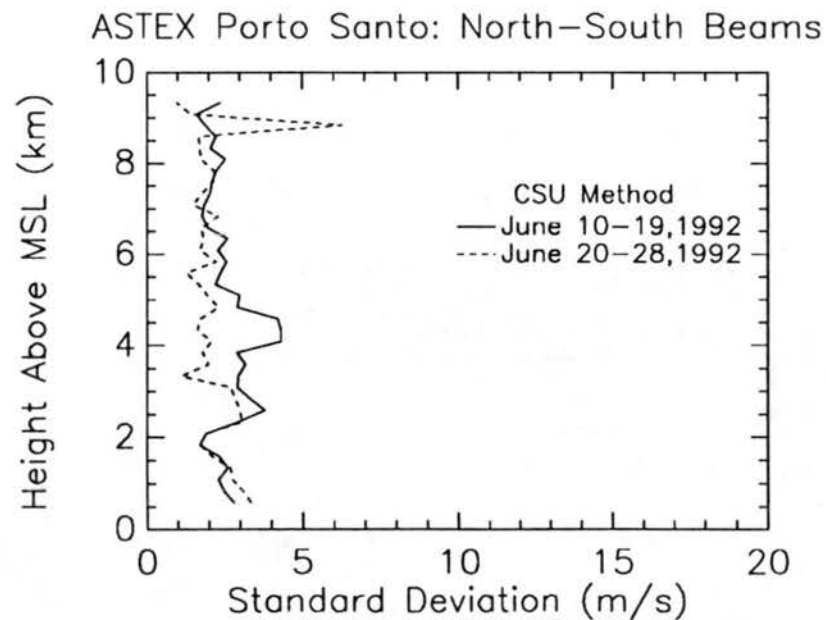
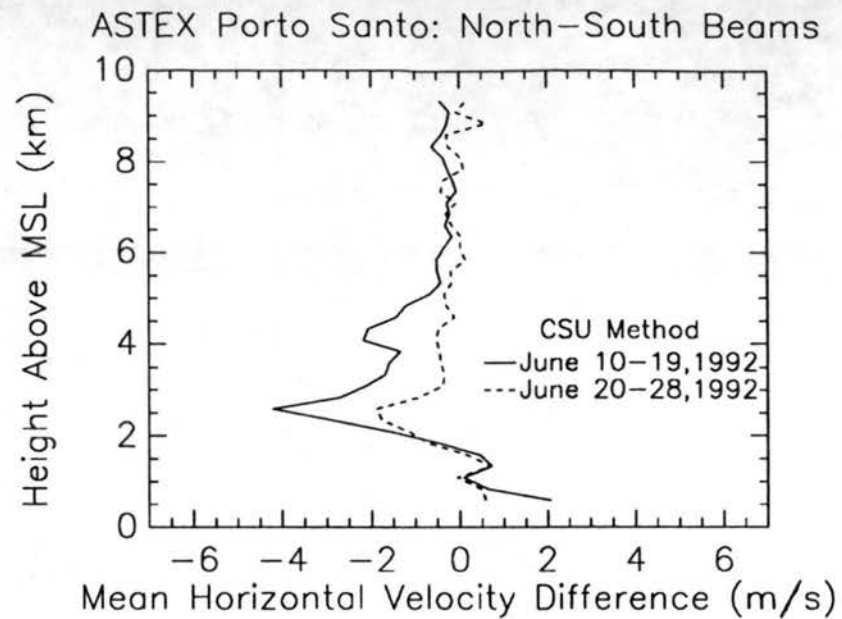
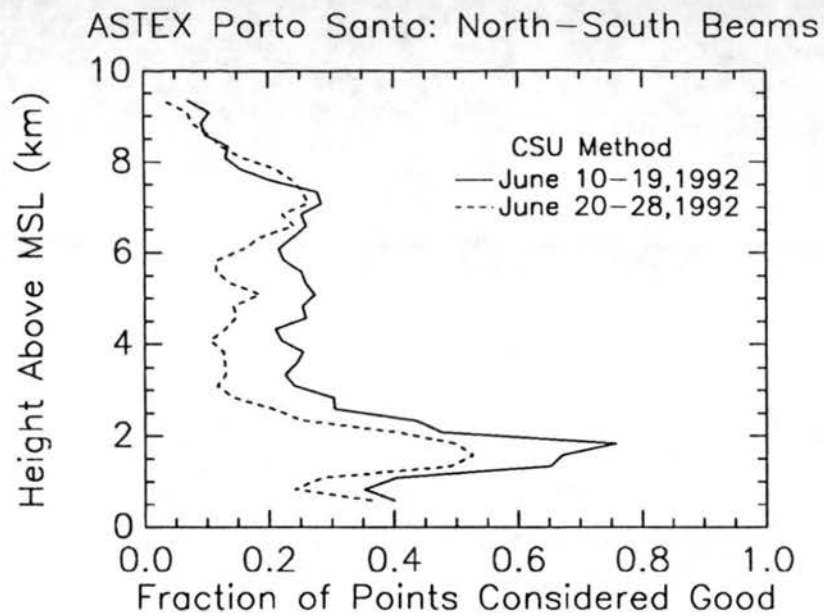


Figure 14. A comparison of the north and south beams using the CSU method on data from Porto Santo.

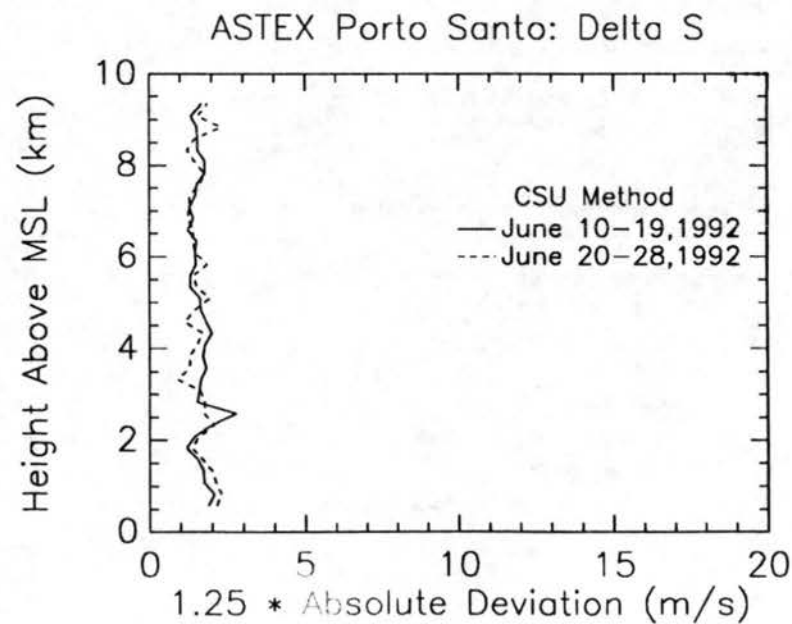
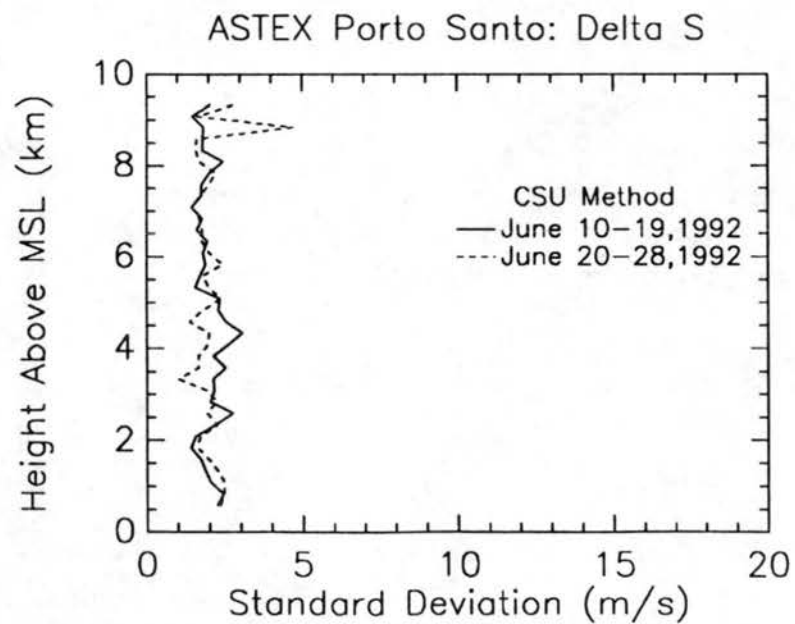
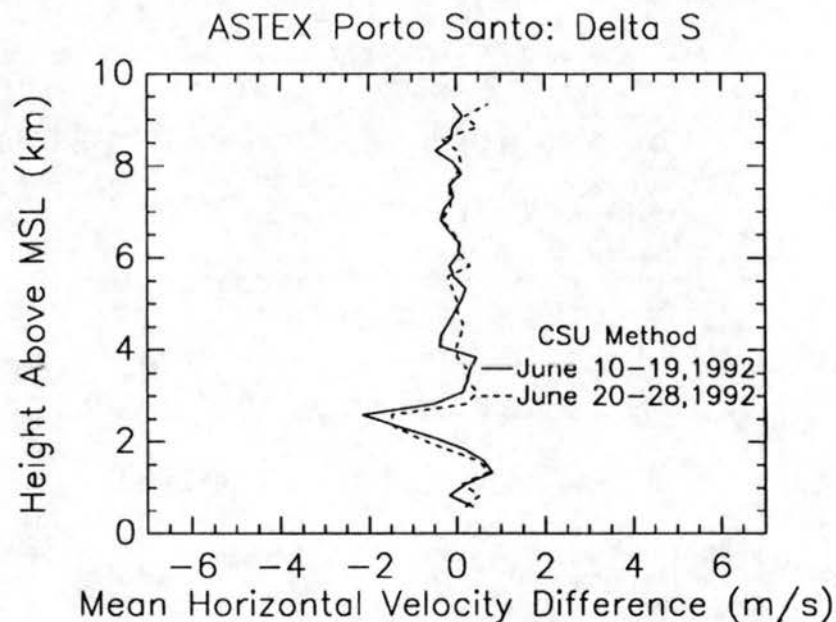
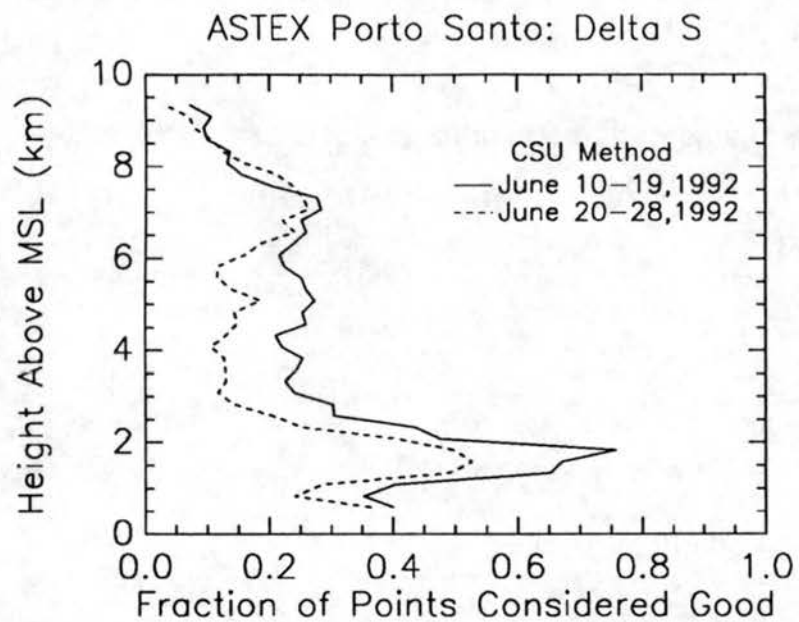


Figure 15. A comparison of beams using the CSU method on data from Porto Santo: ΔS .

4.0 Finding the Correct Peak in the Doppler Spectrum

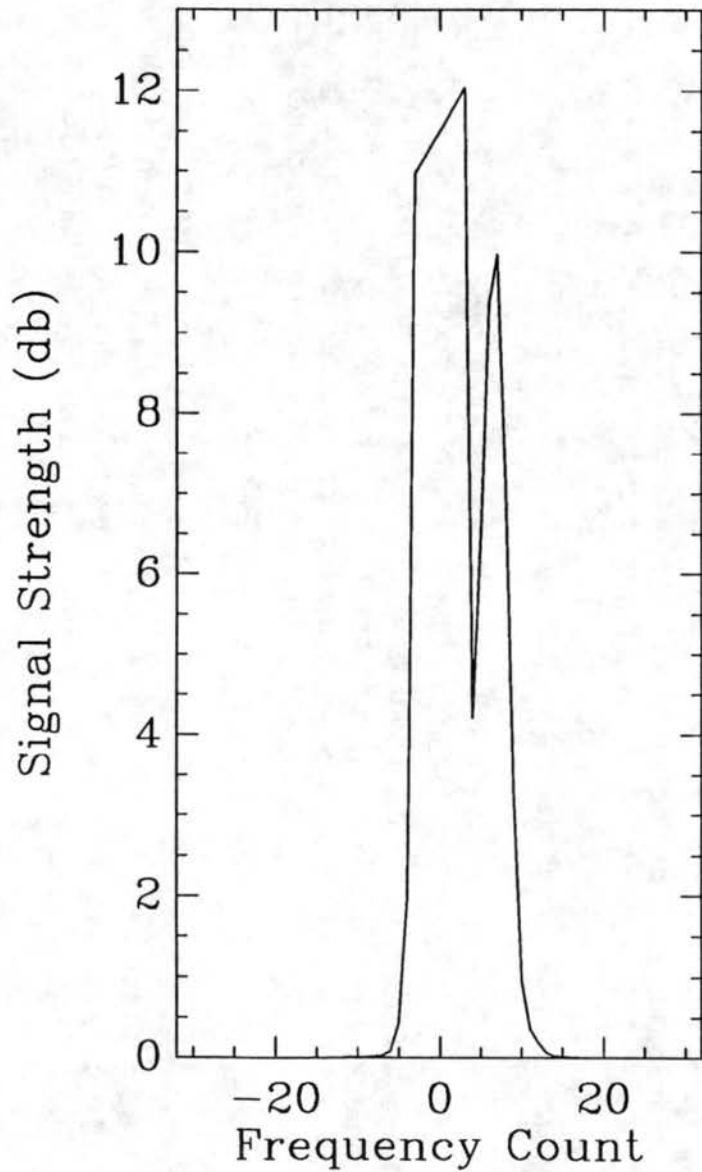
Much of the quality control that needs to be performed can be eliminated if the correct peak in the doppler spectrum is chosen. The results above are from radial velocities determined from the software furnished by the wind profiler manufacturer. This software chooses the highest peak in the center part (about 50%) of the spectrum, and finds a signal-weighted average frequency (SWAF) of the peak, which is then converted into a radial velocity. Unfortunately in many instances the highest peak may be a system noise spike or a partially removed ground clutter peak. If the raw doppler spectrum is available, a more sophisticated signal processing can be used.

A more refined peak finding algorithm, the multi-pass peak finder algorithm (MPPF), has been developed. This algorithm makes use of the surrounding spectra in the profile to help determine the correct peak. First the peaks in the profile are found according to the above SWAF algorithm. This data set of peaks is then used to determine at a particular height the correct (small) section of the spectrum to analyze for a more refined value. This is done by sorting the 11 peaks centered around the height in question and removing 3 peaks from each end of sorted set. This is repeated for 7 peaks (centered around the height in question) with 2 peaks from each end being removed and it is repeated again for 5 peaks with 1 peak from each end being removed. The median of the set of remaining 9 peaks becomes the center point of a small section of the spectrum around where the highest peak in that section will be chosen and processed by the SWAF algorithm. By removing the peaks at the ends of the sort list, possible outlying data points are removed. By repeating this three times over a shorter height interval each time, the peaks near the height in question receive extra weighting. If the peak at the height in question was one of the outlying data points it likely would not have made the cut (even though it would have been given three tries) and would not have been found as the median. The median gives the algorithm a place to look based on continuity with height without being influenced by outliers. The SWAF algorithm is then used on this smaller section that was selected by the median to find the doppler frequency peak.

The ground clutter peak in the original algorithm (of use) is chopped off, assuming a width of 5 or 7 spectral points for the peak. A ground clutter removal algorithm developed at CSU removes the entire ground clutter peak, leaving behind only the obvious peaks embedded in the ground clutter peak. Figure 16 graphically illustrates both methods. Many of the false peaks come from only partially removing the ground clutter peak. The CSU peak removal algorithm removes the entire ground clutter peak but may end up removing more than just ground clutter.

The effectiveness of these methods is demonstrated in three different case studies where the spectra were processed by the standard SWAF method, the SWAF method with the new center peak removal algorithm (NCPR), the new peak finding method (MPPF) with the standard center peak removal algorithm (SCPR), and MPPF with NCPR. To further

Std Center Peak Removal



New Center Peak Removal

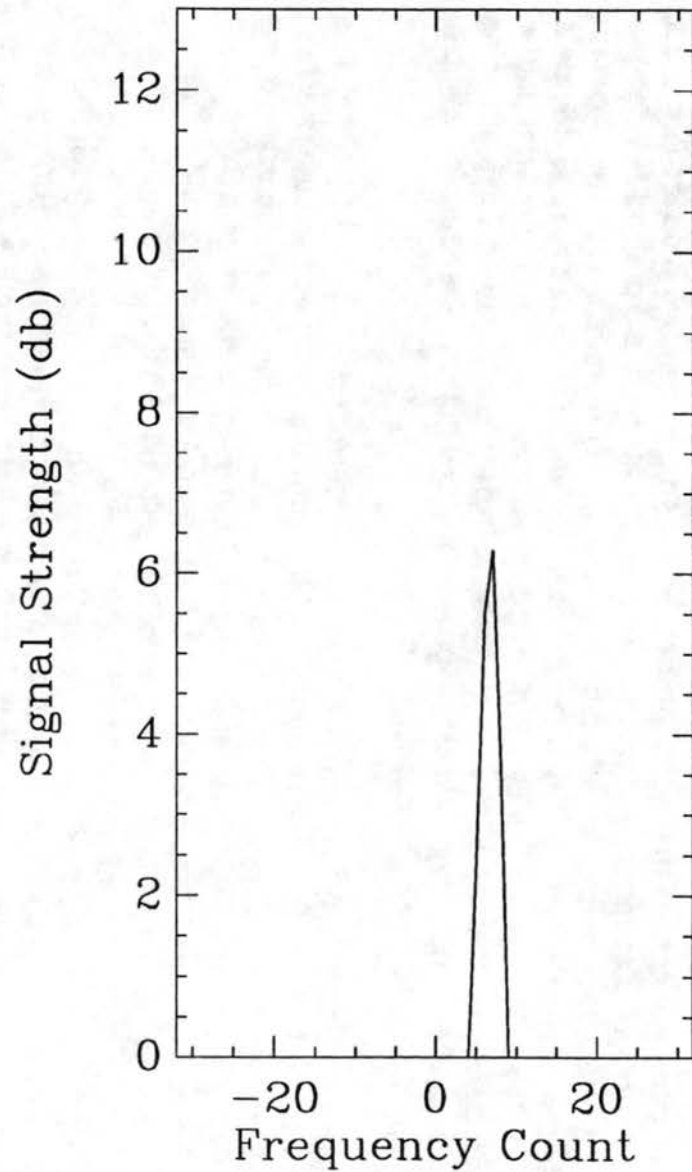


Figure 16. The standard peak removal can leave much of the center peak there. The new method of removing the center peak will remove all the center peak, while leaving the only the obvious embedded peaks.

illustrate the effectiveness of the methods, if the difference between the chosen radial velocities ($\text{abs}(V_{re} + V_{rw})$ or $\text{abs}(V_{rm} + V_{rs})$) are greater than 2 m/s then the processing method has failed and a small triangle is plotted instead (otherwise the data point is considered valid and the two corresponding velocity components are averaged together). Note that strong vertical velocities and side lobe returns also affect the difference. Table 6 for each case and for each of the methods displays the fraction of data where the opposing beams radial velocities are in disagreement or the unexpected null winds (wind speed is less than 2.5 m/s) are found.

The first case (Figure 17), 31 March 1991, depicts a high wind case at the Fort Collins site. MPPF with the SCPR (Figure 17c) showed no improvement over the standard method (Figure 17a) with some improvement seen in MPPF with the NCPR (Figure 17d). No improvement was seen when the NCPR and the standard peak finding method (Figure 17b) were combined. MPPF with SCPR showed many more points with the problem null winds than MPPF with NCPR. These null winds result from a wide center peak caused by side lobe reflections of moving trees and brush on the nearby hillsides. Because the side lobes vary from beam to beam, none of the methods did a very good job of finding the same radial velocity for its opposing beam.

The 23 November 1991 data (Figure 18) are from Parsons, KS. In this case the standard method (Figure 18a) did fairly well. Again processing the data with the standard method and NCPR (Figure 18b) showed no improvement, but when processed with MPPF (Figures 18c,d) significant improvement was seen. MPPF with the SCPR (Figure 18c) again found more null winds than with the NCPR (Figure 18d). The disagreement between beams at the lower levels was seen in the results from the previous section and is likely due to side lobe reflection.

Table 6.

Fraction of points with disagreement between opposing beams or null winds			
Method Used	31 March 1991	23 November 1991	26 November 1991
Standard Method with SCPR	0.76	0.33	0.66
Standard Method with NCPR	0.76	0.33	0.66
MPPF with SCPR	0.77	0.21	0.38
MPPF with NCPR	0.72	0.18	0.38

CSU Wind Profiler: 910331 Std Center Peak Removal

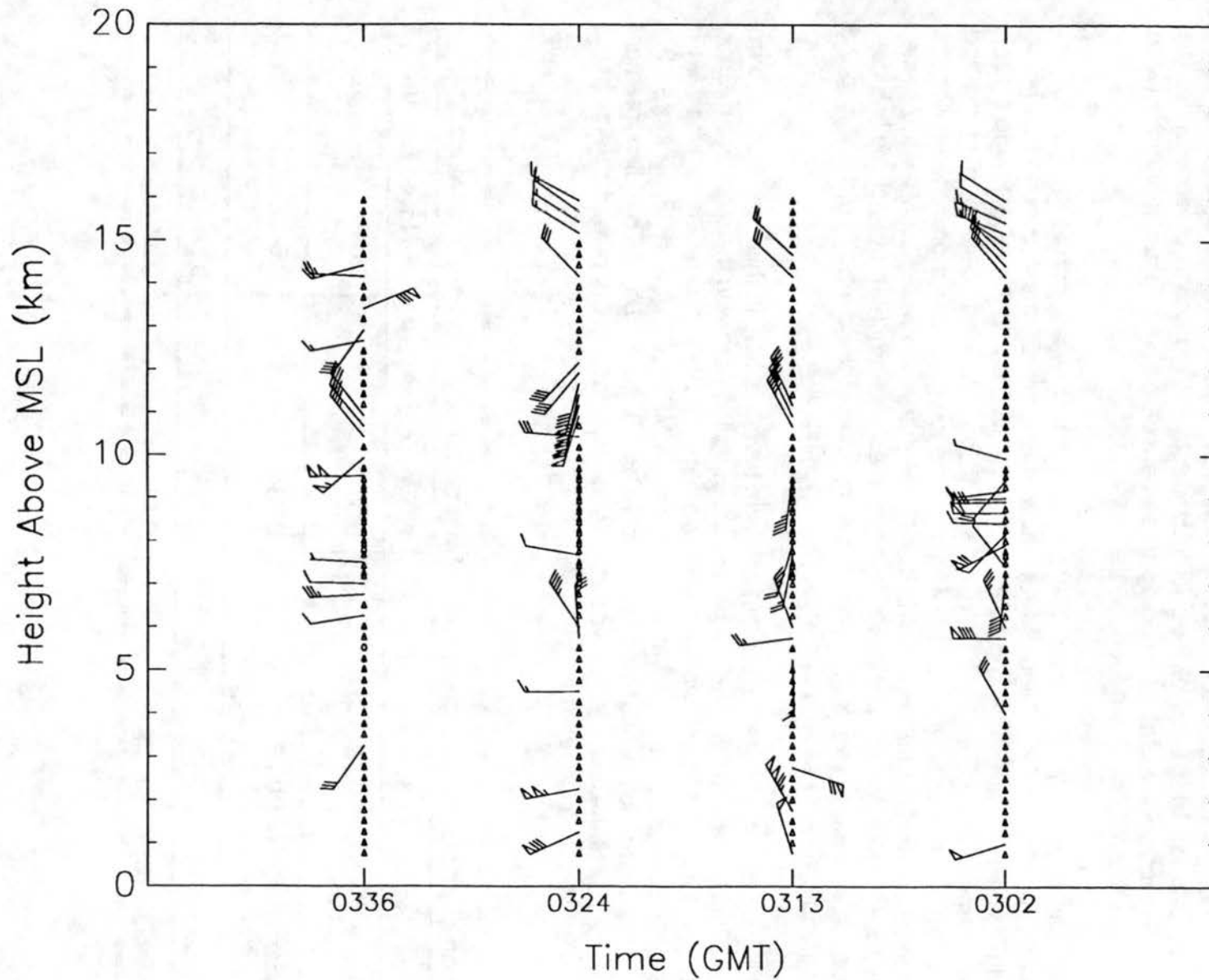


Figure 17a. High wind case on 31 March 1991: Spectra processed by the standard method with standard center peak removal.

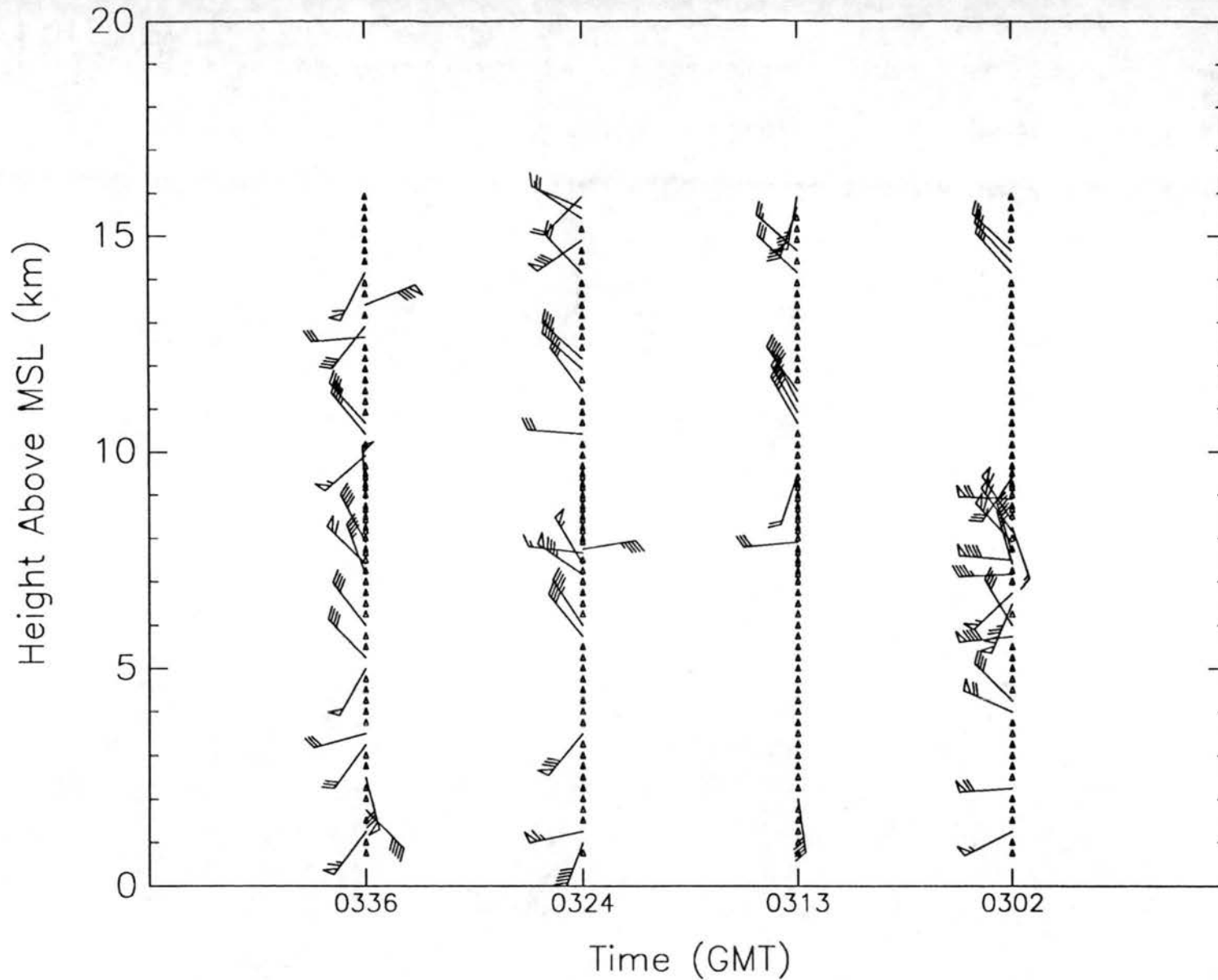


Figure 17b. High wind case on 31 March 1991: Spectra processed by the standard method with the new center peak removal method.

CSU Wind Profiler: 910331 New Method SPR

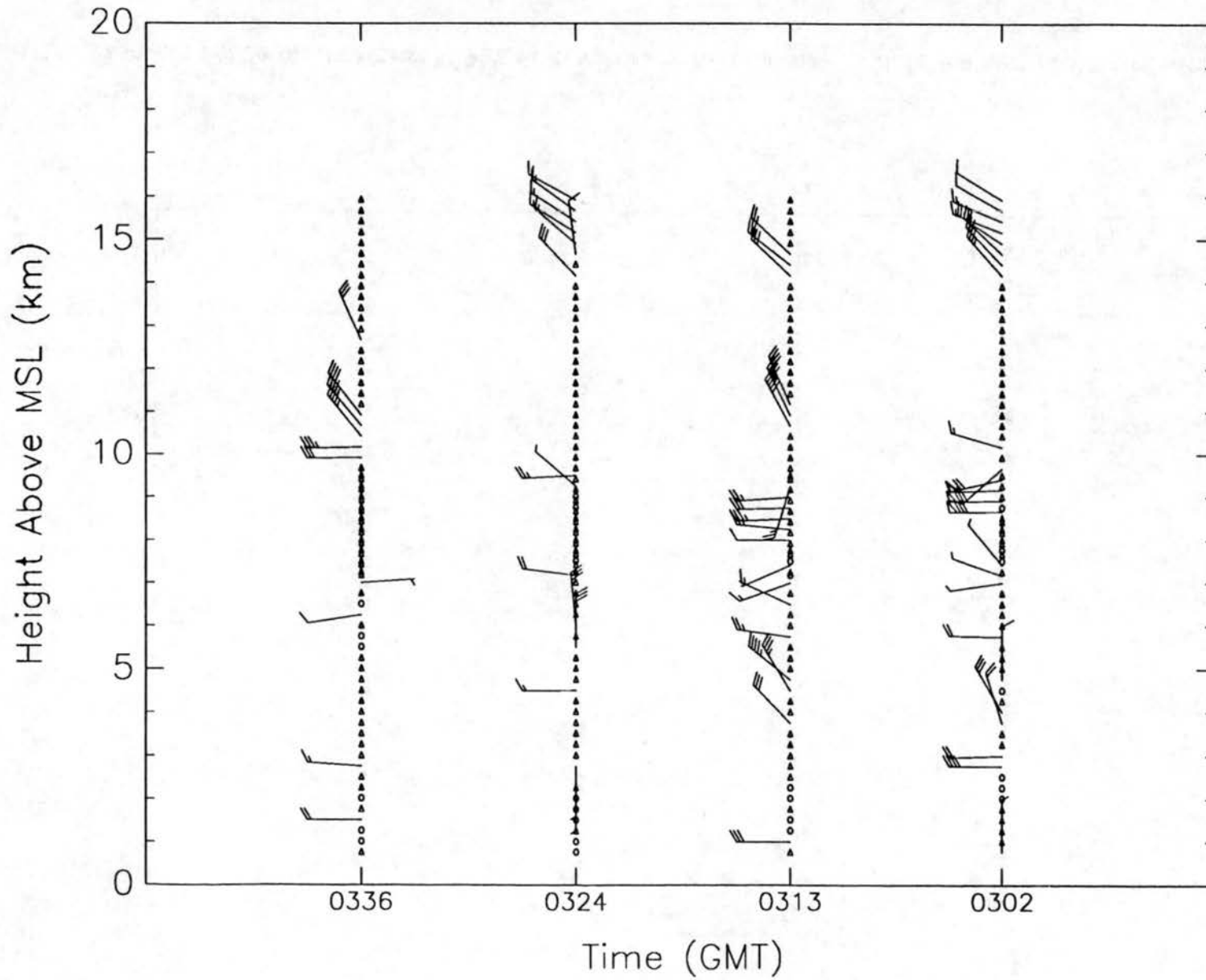


Figure 17c. High wind case on 31 March 1991: Spectra processed by the new method with standard center peak removal.

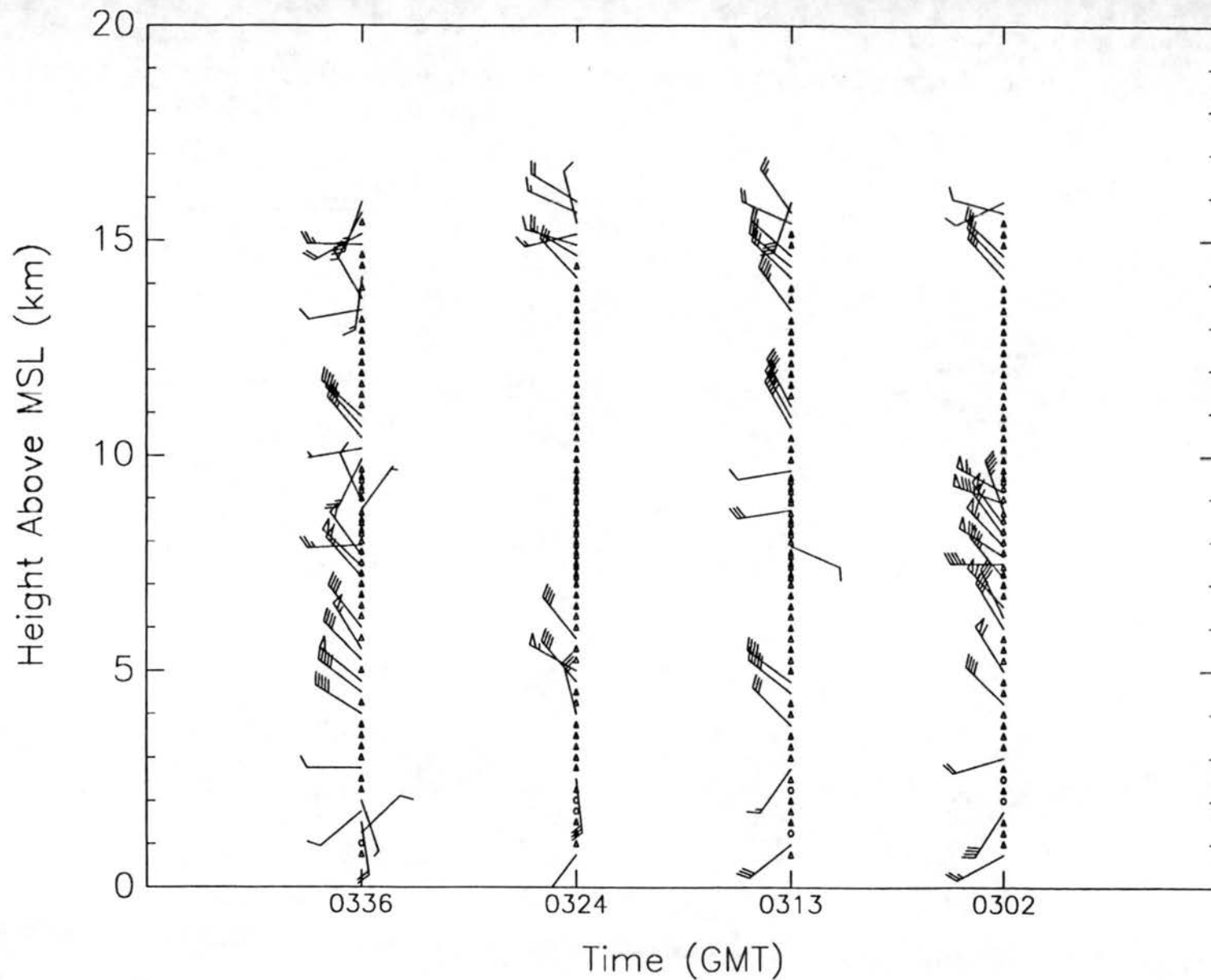


Figure 17d. High wind case on 31 March 1991: Spectra processed by the new method with the new center peak removal method.

CSU Wind Profiler: 911123 Std Center Peak Removal

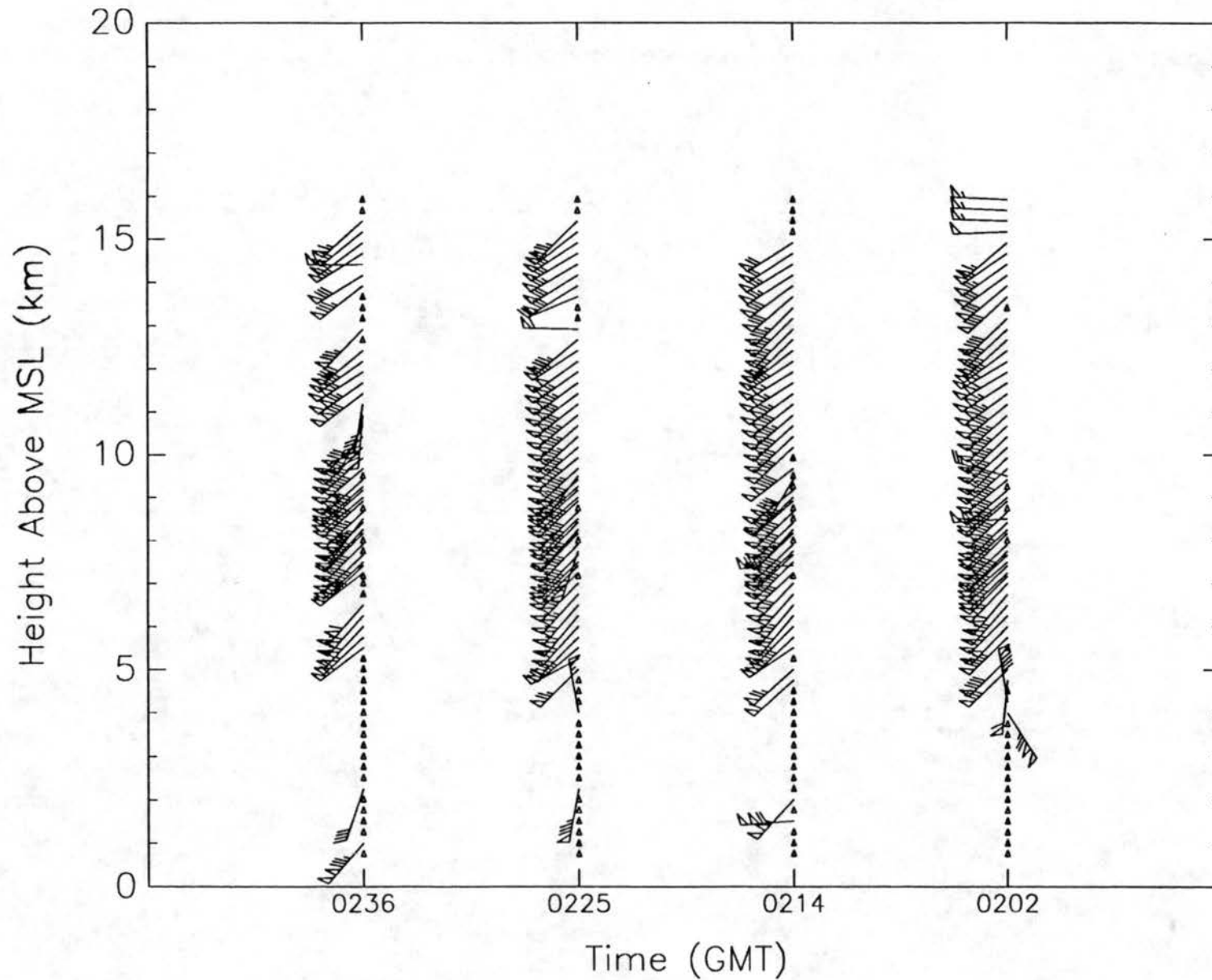


Figure 18a. Typical case on 23 November 1991: Spectra processed by the standard method with standard center peak removal.

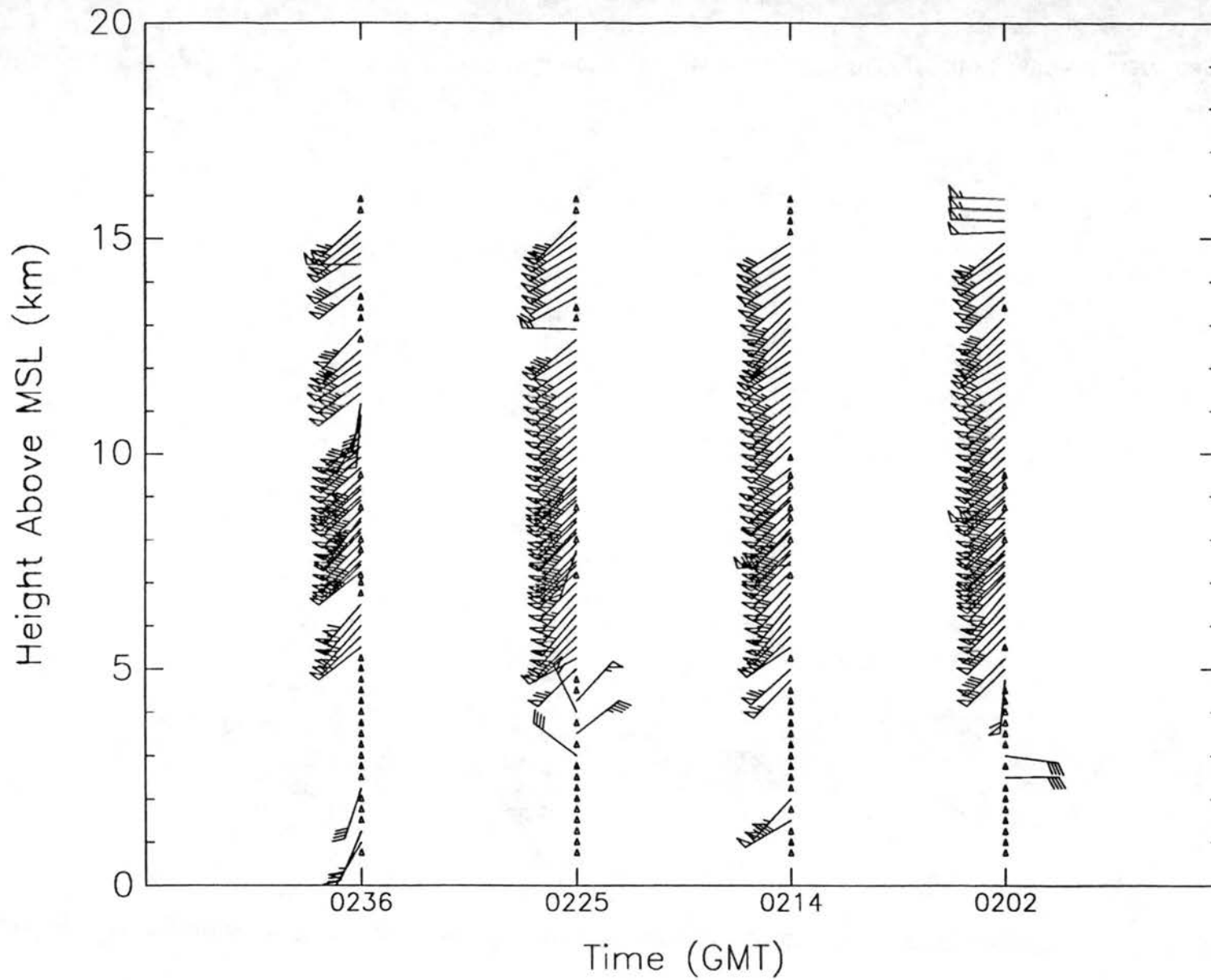


Figure 18b. Typical case on 23 November 1991: Spectra processed by the standard method with the new center peak removal method.

CSU Wind Profiler: 911123 New Method SPR

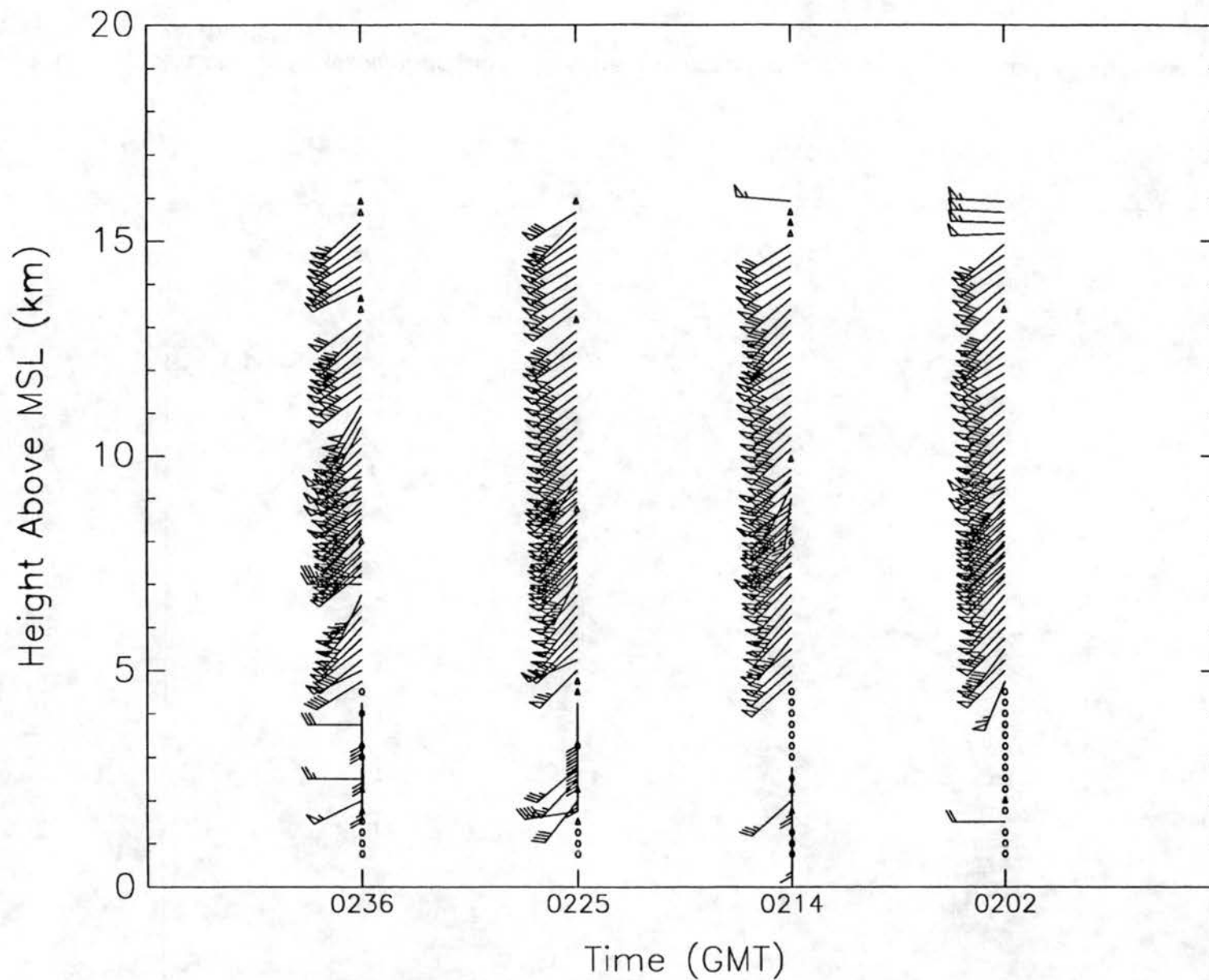


Figure 18c. Typical case on 23 November 1991: Spectra processed by the new method with standard center peak removal.

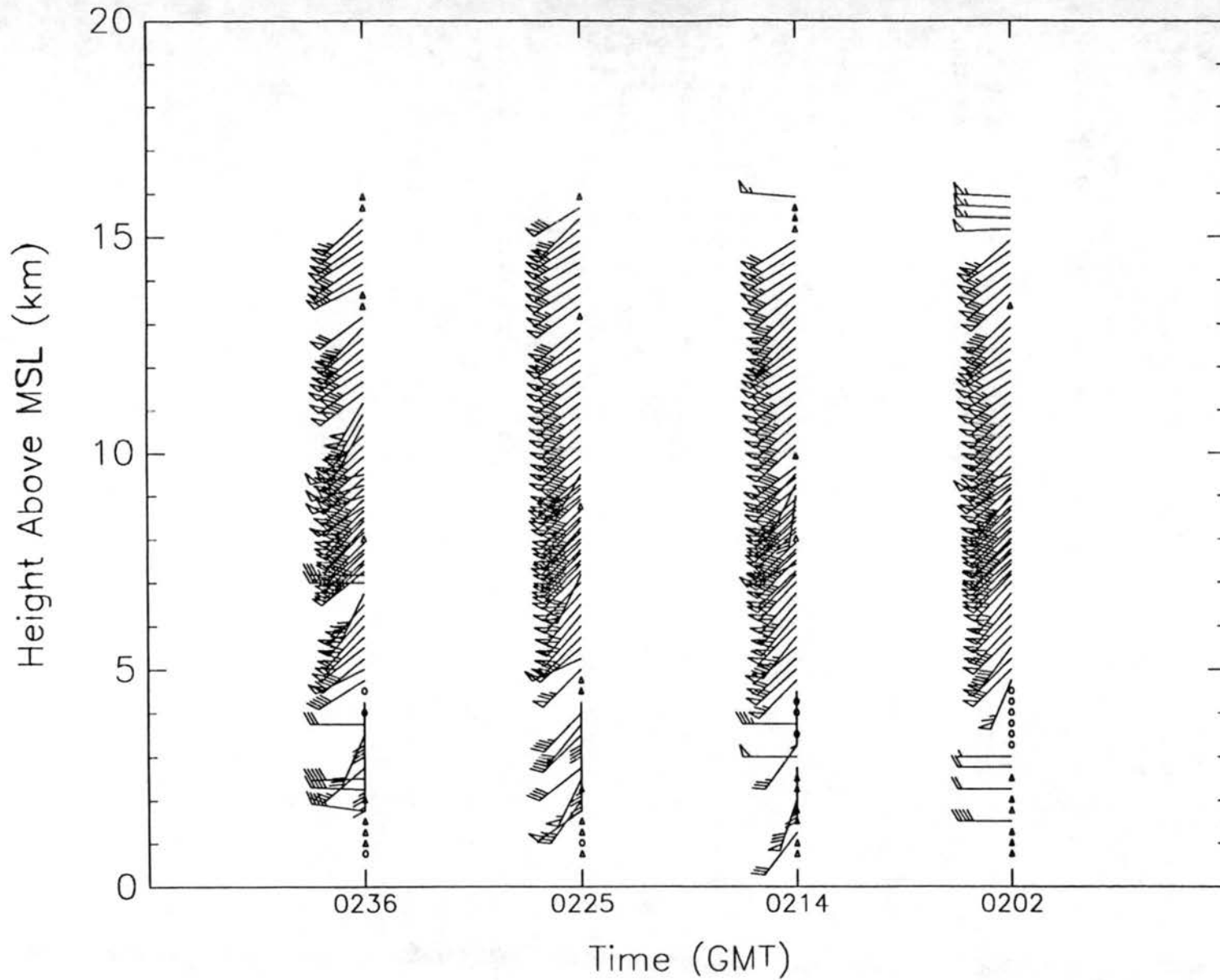


Figure 18d. Typical case on 23 November 1991: Spectra processed by the new method with the new center peak removal method.

The third case, 26 November 1993, (Figure 19) is also from Parsons, KS. The standard case (Figure 19a) again did fairly well but this time several good west winds were removed when the data were processed with NCPR (Figure 19b). The center peak of the north and south beams had also contained the northward velocity component. In this case too much of the center peak was removed. This also adversely affected the performance of MPPF with NCPR (Figure 19d). Though the fractional disagreement between beams, as shown in Table 6, seems to be unaffected by the center peak removal method, many questionable winds appeared when the NCPR is used. Because the northward velocity component was embedded in the center peak, the MPPF with SCPR (Figure 19c) performed the best in this case.

The new peak finding method (MPPF) clearly performed better than the standard SWAF method and usually combining MPPF with the NCPR allow for even more improvement.

5.0 Concluding Remarks

The continuity method of Weber and Wuertz performed the best of all the quality control methods. Using the standard deviation of ΔS as a measure of relative accuracy of the CSU wind profiler then the profiler horizontal winds appear to be accurate to about 3 m/s (discounting any bias) with one third of the data being rejected. However the accuracy can likely be improved by using more sophisticated peak finding algorithms on the doppler spectra as shown in Section 4. Perhaps combining the more sophisticated signal processing with the continuity method will give the greatest improvement in the quality of the CSU wind profiler data. Ultimately the improved accuracy of the wind profiler will come from improved signal processing of the doppler spectra.

Acknowledgements. We would like to acknowledge the help and support of John Davis, Dave Wood and Chris Cornwall, who were instrumental in maintaining the wind profiler in a continuous operational state. Our thanks also goes out to Melissa Tucker for her assistance in the preparation of this document. This research has been supported by the Office of Naval Research under contract No. N00014-91-J-1422, P00002, and the National Aeronautics and Space Administration under grant NAG 1-1146.

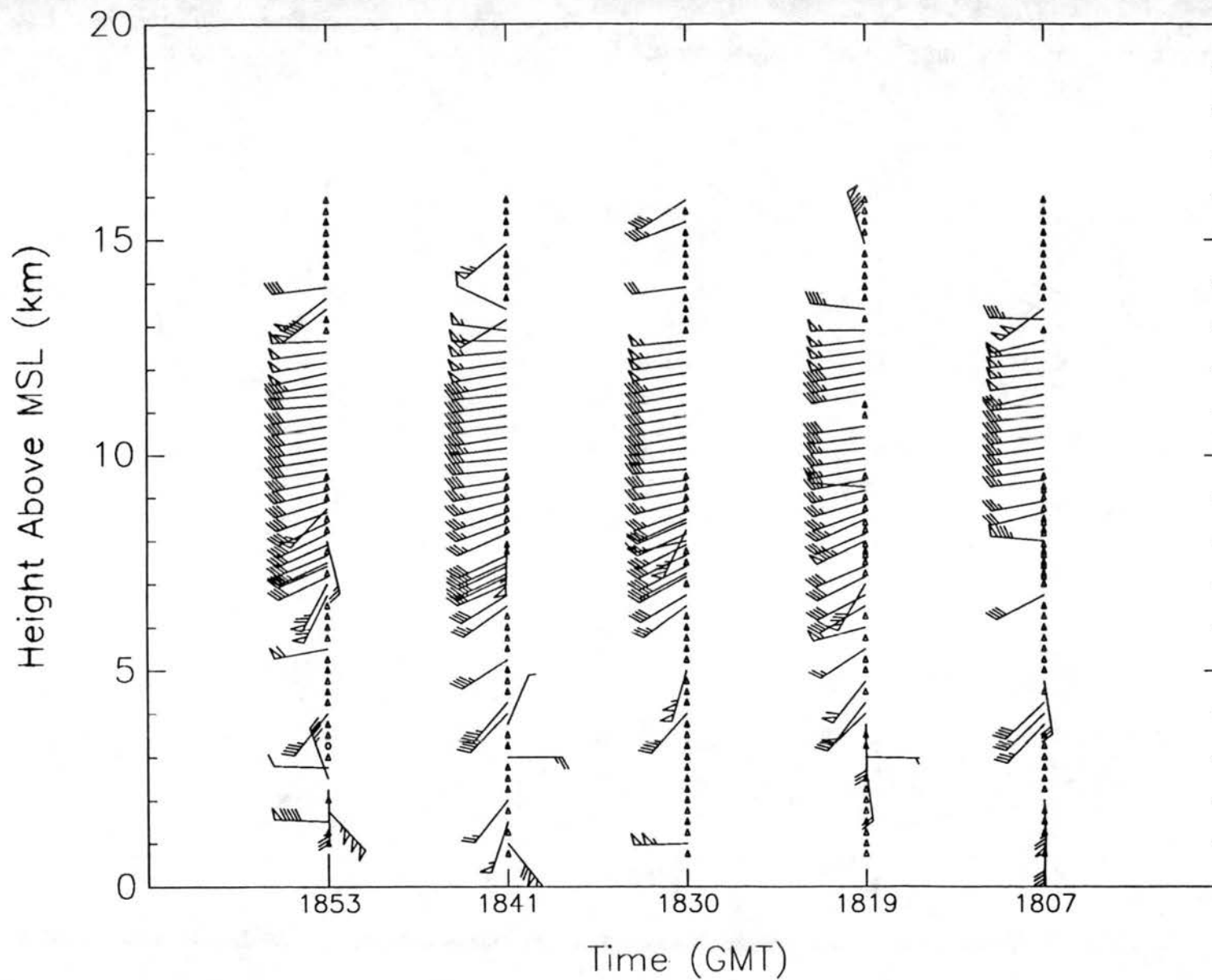


Figure 19a. A west wind case on 26 November 1991: Spectra processed by the standard method with standard center peak removal.

CSU Wind Profiler: 911126 New Center Peak Removal

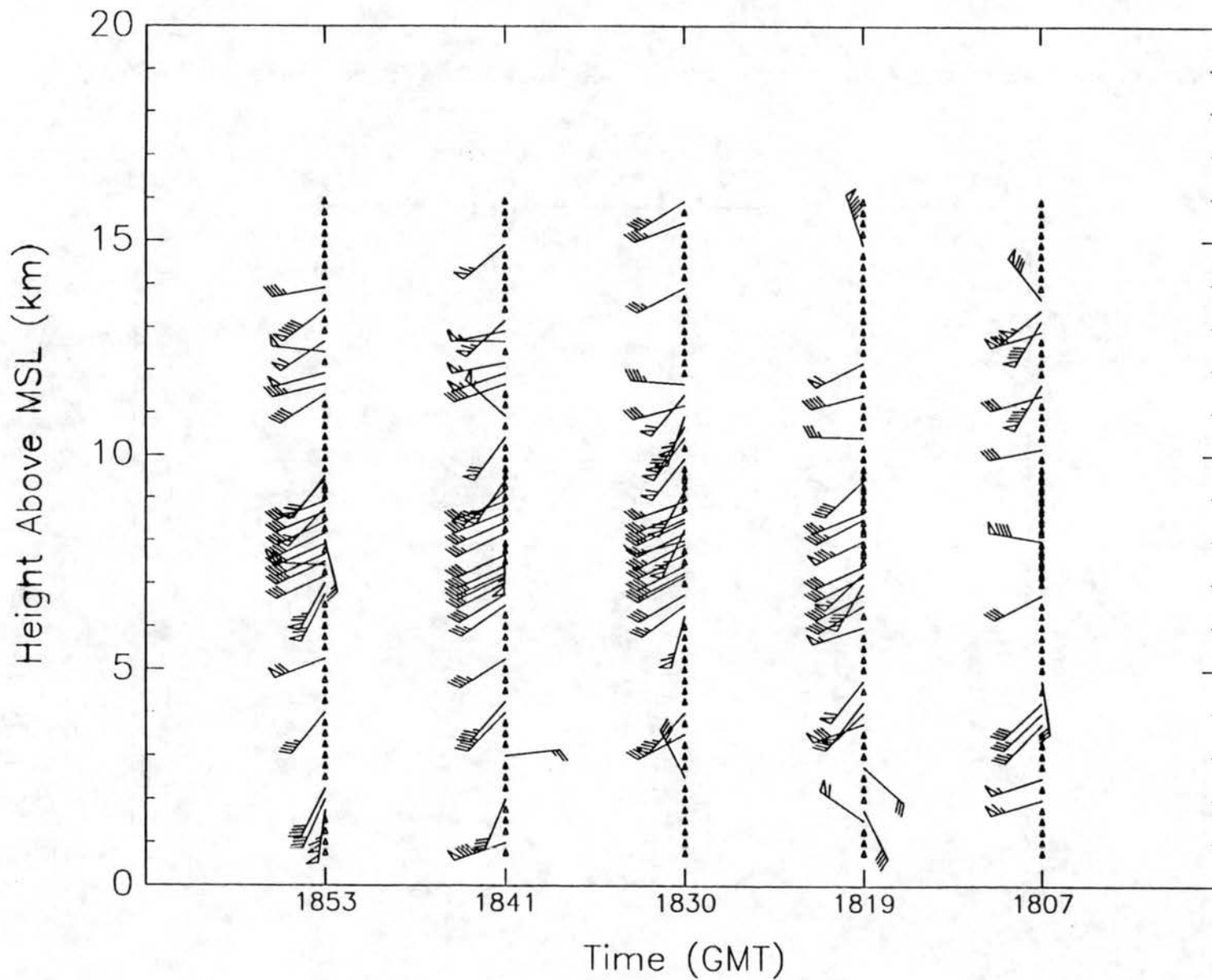


Figure 19b. A west wind case on 26 November 1991: Spectra processed by the standard method with the new center peak removal method.

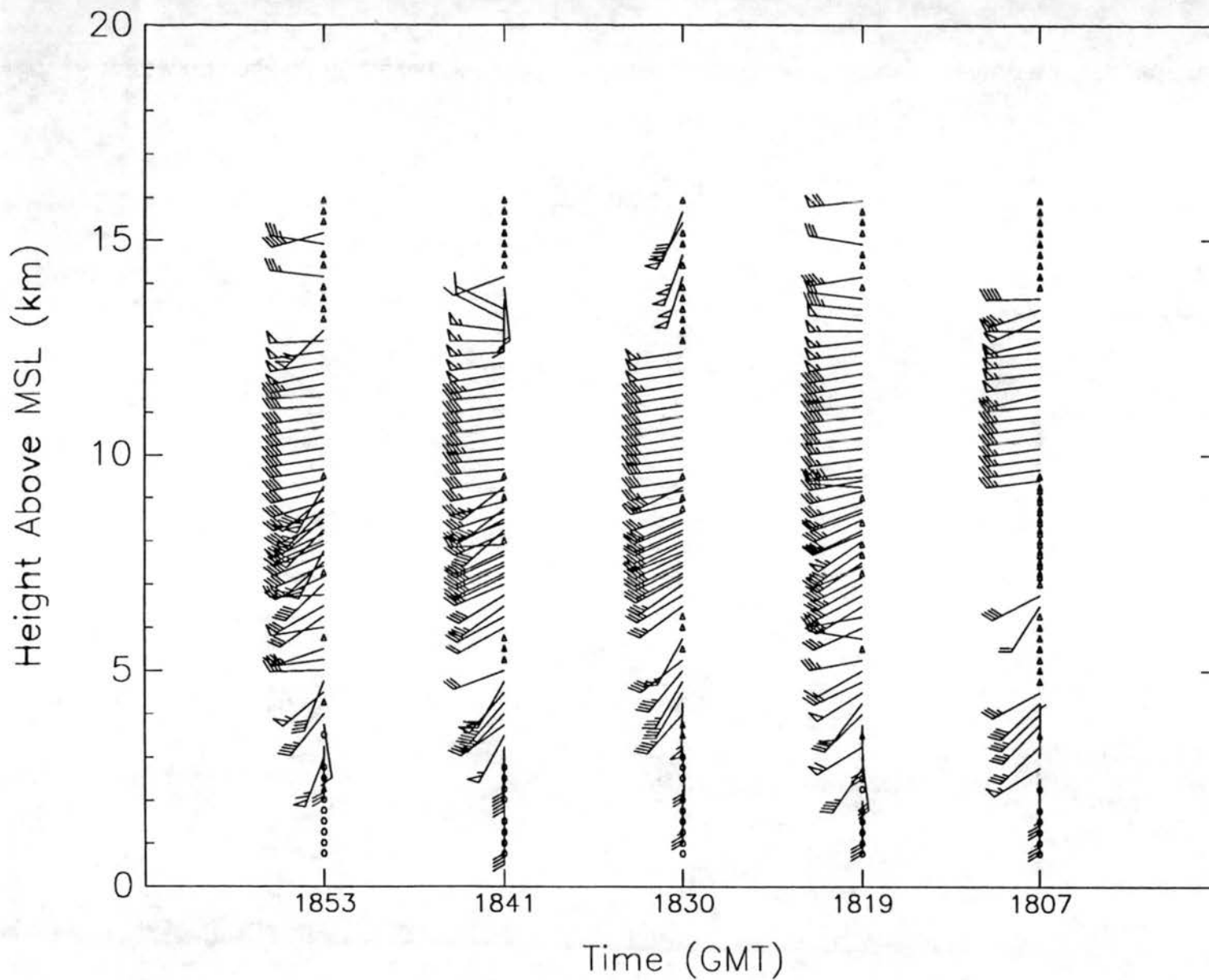


Figure 19c. A west wind case on 26 November 1991: Spectra processed by the new method with standard center peak removal.

CSU Wind Profiler: 911126 New Method

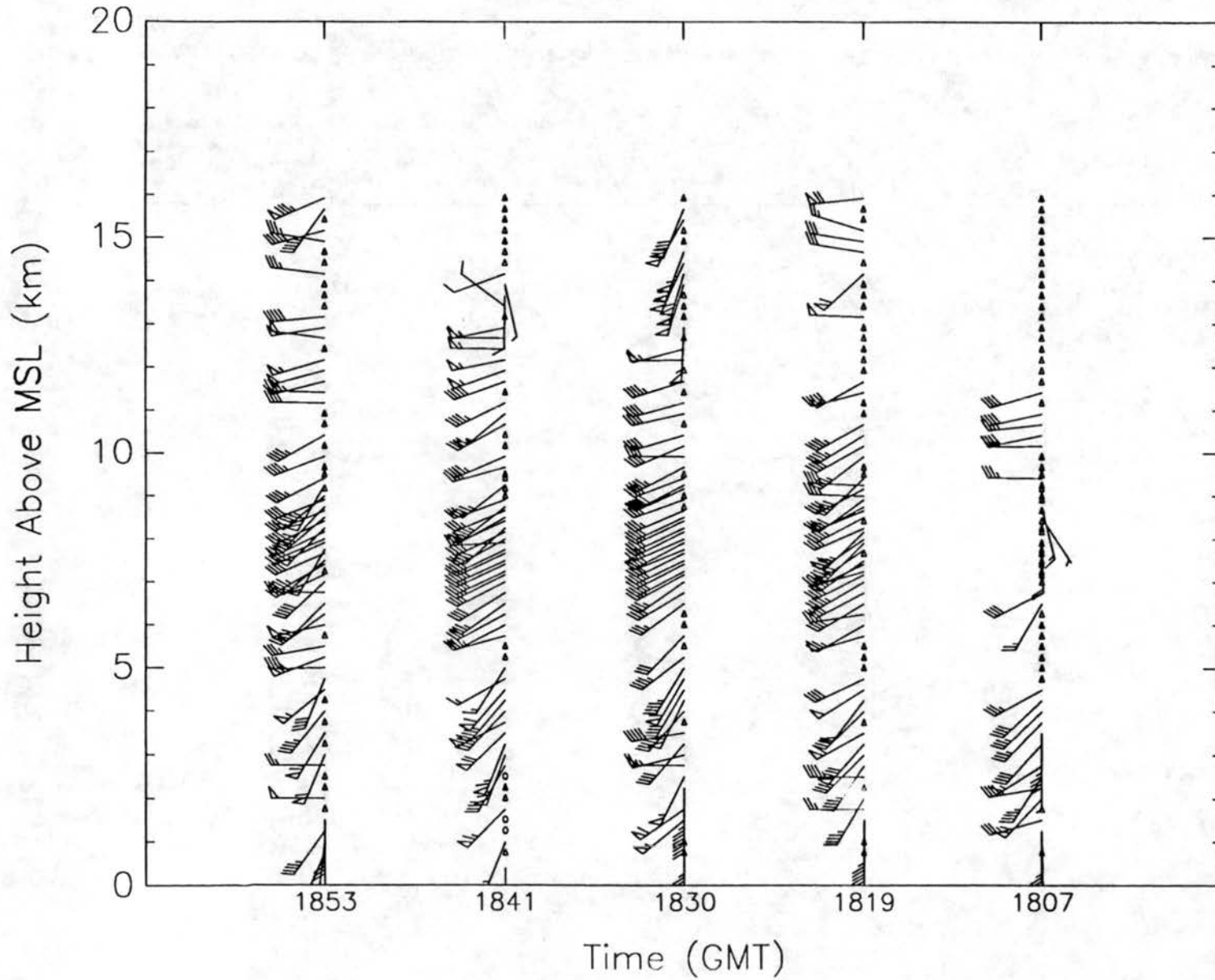


Figure 19d. A west wind case on 26 November 1991: Spectra processed by the new method with the new center peak

References

- Brewster, K. A., 1989: Quality control of wind profiler data. Profiler Training Manual 2. NOAA/ERL/FSL, Boulder, CO, 39 pp.
- , and T. W. Schlatter, 1988: Recent progress in automated quality control of wind profiler data. Preprints, *8th Conference on Numerical Weather Prediction*, Baltimore, Amer. Meteor. Soc., 331-338.
- Cox, S., C. Cornwall, W. Cotton, J. Davis, J. Kleist, T. McKee, Q. Shao, D. Randall, W. Schubert, D. Wood, S. Frisch, M. Hardesty, R. Kropfli, J. Snider, P. Anikin, 1993: CSU/NOAA-WPL FIRE II - ASTEX field experiment: Description of field deployment phase. *Atmos. Sci. Pap. No. 523*, Colorado State University, Ft. Collins, 100 pp.
- , G. Beck, C. Cornwall, J. Davis, P. Hein, C. Lappen, R. Song, J. Withrow, and D. Wood, 1992: CSU FIRE II cirrus field experiment: Description of field deployment phase: FIRE Series No. 8. *Atmos. Sci. Pap. No. 506*, Colorado State University, Ft. Collins, 79 pp.
- Fischler, Martin A., and Robert C. Bolles, 1981: Random sample consensus: A paradigm for model fitting with applications to image analysis and automated cartography. *Commun. Assoc. Comput. Mach.*, **24**, 381-395.
- Hein, Paul F., John M. Davis, and Stephen K. Cox, 1991: Quality Control of the CSU wind profiler data. *Lower Tropospheric Profiling: Needs and Technologies*, 131-132.
- Strauch, R. G., B. L. Weber, A. S. Frisch, C. G. Little, D. A. Merrit, K. P. Moran, and D. C. Welsh, 1987: The precision and relative accuracy of profiler wind measurements. *J. Atmos. Oceanic Technol.*, **4**, 563-571.
- Weber, B. L., D. B. Wuertz, and D. C. Welsh, 1993: Quality controls for profiler measurements of winds and RASS temperatures. *J. Atmos. Oceanic Technol.*, **10**, 452-464.
- , and D. B. Wuertz, 1991: Quality control algorithm for profiler measurements of winds and RASS temperatures. NOAA Tech. Memo., ERL WPL-212, 32 pp.

948233 ST